2015•2016
FACULTEIT GENEESKUNDE EN LEVENSWETENSCHAPPEN
master in de biomedische wetenschappen

Masterproef

Star polymers for biomedical application

Promotor :
Prof. dr. Thomas JUNKERS

Jeroen Vrijsen

Scriptie ingediend tot het behalen van de graad van master in de biomedische wetenschappen

De transnationale Universiteit Limburg is een uniek samenwerkingsverband van twee universiteiten in twee landen: de Universiteit Hasselt en Maastricht University.

universiteit hasselt
KNOWLEDGE IN ACTION

Universiteit Hasselt | Campus Hasselt | Martelarenlaan 42 | BE-3500 Hasselt
Universiteit Hasselt | Campus Diepenbeek | Agoralaan Gebouw D | BE-3590 Diepenbeek

universiteit hasselt | Maastricht University

2015•2016
FACULTEIT GENEESKUNDE EN LEVENSWETENSCHAPPEN
master in de biomedische wetenschappen

Masterproef

Star polymers for biomedical application

Promotor :
Prof. dr. Thomas JUNKERS

Jeroen Vrijsen
Scriptie ingediend tot het behalen van de graad van master in de biomedische wetenschappen

universiteit hasselt | Maastricht University

Acknowledgements

So here it is, the conclusion of an adventure that started five years ago. When the end is in sight it gives the opportunity to reflect back and appreciate the positive and negative experiences of the past five years. One of the main reasons why I decided to go for scientific studies and aim for a similar career is a healthy portion of curiosity that was sparked in high school. This same curiosity has only grown throughout this journey and will most likely never stop. Soon I will embark on an even bigger adventure to grow even further as a scientist.

But first I would like to thank all the people that made this thesis possible and allowed me to create something I am proud of.

Special thanks go to Professor Thomas Junkers, the promotor of my masterthesis. He gave me the opportunity to develop and conduct my own project in his labs. I enormously appreciate the chances and support he gives me to pursuit a scientific career as well as his patience during the necessary hurdles every young developing scientist has to take.

Thank you as well, Benjamin and Nok. You have been the best daily supervisors I could have hoped for. I could not have done it without you two. You gave me the freedom to explore and perform my project, while also being immediately there for me when I needed your help. I enjoyed working with you and am grateful as well for the fun moments we had after work. I would also like to acknowledge Professor Milos Nesladek, my second examiner, for the time he made to listen to the difficulties and successes I encountered during my project.

I also want to thank everyone from the OBPC group for their help and scientific input. Joke and Evelien, thank you for measuring many ESI-MS samples. Also thank you Joris, Gijs and Neomy for keeping the GPC alive during my project. Again thank you Neomy for the synthesis of MDMO-PPV. I'm also grateful for Gunther and Koen for measuring the countless NMR samples I produced every day. I would also like to thank Oliver, for the fun two months we had during his research stay.

During my studies I also got to know many people which have come to be great friends. Especially Anne, Geoffrey, Jens, Jeroen and Senne, I could not have wished for better friends to have during my studies. Without you guys it would not have been the same, so thank you! Also great thanks to my family and parents who always support me and allowed me to become whatever I wanted to be. And of course, thank you, Kimberly for always being there for me and listening to my endless scientific banter.

Jeroen Vrijsen,

8th of June 2016

Table of Contents

Used Abbreviations

^{1}H-NMR	Proton nuclear magnetic resonance
21BrCD	21-arm initiator
β-CD	β-cyclodextrin
Boc	*tert*-butyloxycarbonyl
$CDCl_3$	Deuterated chloroform
CH-Br	Initiating group
$CH\text{-}N_3$	Azide modified end group
$CH\text{-}NH_2$	primary amine modified end group
CH-phtalimide	polymer end groups containing a phtalimide
CH_2Cl_3	Chloroform
CMC	Critical micelle concentration
CMP	Copper-mediated reversible-deactivation radical polymerization
Cu^0	Copper(0)
Cu^IAAC	Copper(I)-catalyzed alkyne-azide cycloaddition
Cu^IBr	Copper(I)bromide
$Cu^{II}Br_2$	Copper(II)dibromide
Đ	Dispersity
D_{50}	Diameter at 50% of a cumulative distribution
DCM	Dichloromethane
DEGA	Di(ethylene glycol) ethyl ether acrylate
DLS	Dynamic light scattering
DMF	*N,N*-Dimethylformamide
DMSO	Dimethyl sulfoxide
EBiB	Ethyl α-bromoisobutyrate
ESI-MS	Electrospray ionization mass spectrometry
FDA	Food and drug administration
FRP	Free radical polymerization
GPC	Gel permeation chromatography
HCl	Hydrochloric acid
HEA	Hydroxyethyl acrylate

HPLC	High performance liquid chromatography
KOH	Potassium hydroxide
LCST	Lower critical solution temperature
MA	Methyl acrylate
MDMO-PPV	Poly(2-methoxy-5-(3′,7′-dimethyloctyloxy)-1,4-phenylene-vinylene)
Me_6TREN	Tris-(2(dimethylamino)ethyl)amine
$MgSO_4$	Magnesium sulfate
M_n	Number average molecular weight
m/z	Mass/charge
N_3	Azide
$NaHCO_3$	Sodium bicarbonate
NaN_3	Sodium azide
NH_2	Amine
NMP	Nitroxide mediated polymerization
Pd/C	Palladium on activated charcoal
pDEGA	poly(di(ethylene glycol) ethyl ether acrylate)
PFA	Perfluoroalkoxy
photoCMP	photo-initiated copper-mediated reversible-deactivation radical polymerization
pMA	Poly(methyl acrylate)
PMDETA	*N,N,N′,N′′,N′′*-Pentamethyldiethylenetriamine
pNIPAM	poly(N-isopropylacrylamide)
PPh_3	Triphenylphosphine
PS	Polystyrene
RAFT	Reversible addition-fragmentation chain transfer
RDRP	Reversible-deactivation radical polymerization
TEA	Triethylamine
THF	Tetrahydrofuran
UCST	Upper critical solution temperature
UV	Ultraviolet
UV-VIS	Ultraviolet-visible light

Abstract

Star polymers are structures composed of a central core from which various polymer chains, called arms, extend. These macromolecules can be synthesized using reversible-deactivation radical polymerization techniques which allow high control over the size, shape and composition of the polymer. Hence, the creation of highly defined star shaped polymers became possible. These unique structures possess abundant functional groups, possible stimuli-responsive capacity, outstanding structural stability and the potential to encapsulate hydrophobic drugs. All of these properties are of major interest in the field of nanomedicine. Efficient solutions to improve current treatments such as cancer therapy are developed in this interdisciplinary research domain. Therefore the continued development of star shaped structures will definitely have a beneficial impact on this field.

In this thesis star polymers with up to 21 arms were synthesized with the core first approach using photo-initiated copper-mediated reversible-deactivation radical polymerization. β-cyclodextrin was selected as central core molecule. It was possible to synthesize these star polymers both in batch as well as in continuous flow reactors. Composing the arms out of an inner methyl acrylate block and di(ethylene glycol)ethyl ether acrylate as outer block was explored. The former serves as inner hydrophobic layer while the latter introduces a temperature-responsive property in the star polymer. During chain extension also a low molecular weight distribution was observed. This indicated that further optimization of the diblock synthesis procedure has to be performed during future research. Regardless, a temperature response was observed occurring around 14 °C.

The star polymers possess high end group fidelity as a consequence of the polymerization technique. The introduction of various useful chemical moieties such as an azide and amine end group was investigated on linear polymers in the second part of the thesis. Translation of the azide end group modification strategy to star polymers was investigated as well. In a preliminary experiment the attachment of poly(*p*-phenylene vinylene) polymers to these azide end group modified star polymers was tested. In the final part, a brief drug loading experiment was performed investigating the potential of the star polymer for future drug delivery experiments. Herein, complex self-assembly of the star polymer can be expected which could aid drug loading.

The possible temperature-responsive property together with the promising first indications on the drug loading potential stimulates the conduction of future detailed investigations regarding drug entrapment and controlled drug release once optimized. Furthermore, the correct implementation of fluorescent PPVs will enable the future use of star polymers for (bio)imaging purposes. The current work therefore made a first step upon which future investigations can be build up.

Nederlandse Samenvatting

Ster polymeren zijn structuren opgebouwd uit een centrale kern van waaruit zich meerdere polymeer ketens uitstrekken. Deze macromoleculen kunnen gesynthetiseerd worden via reversibele-deactivatie radicalaire polymerisatie technieken die een sterke controle over de grootte, vorm en compositie van het polymeer bieden. De gevormde structuren bezitten een overvloed aan functionele groepen, potentiële stimuligevoelige capaciteiten, uitzonderlijke structurele stabiliteit en de mogelijkheid om een hydrofobe drug op te nemen. Al deze eigenschappen zijn zeer interessant voor het veld nanomedicine waarin efficiënte oplossingen worden ontwikkeld om huidige behandelingen zoals kankertherapie te verbeteren. Daaromtrent zal de verdere ontwikkeling van deze stervormige structuren ongetwijfeld een voordelige bijdrage leveren aan dit veld.

In deze thesis werden sterpolymeren met maximum 21 armen gesynthetiseerd door middel van licht-geïnitieerde koper-gemedieerde reversibele-deactivatie radicalaire polymerisatie via een 'kern eerst' methode. β-cyclodextrine werd geselecteerd als kern molecule. Het was mogelijk deze ster polymeren te synthetiseren in zowel batch als continue flow reactoren. De opbouw van de armen uit een binnenste methyl acrylaat blok en di(ethyleen glycol)ethyl ether acrylaat als buitenste blok was verkend. Het eerste blok fungeert als hydrofobe portie terwijl het laatste een temperatuurgevoelige eigenschap in het ster polymeer inbouwt. Tijdens ketenverlenging werd ook een verdeling van laag moleculair gewicht geobserveerd. Hieruit kan worden afgeleid dat verder optimalisatie van de diblock syntheseprocedure moet worden uitgevoerd. Ongeacht werd er toch een temperatuurrespons geobserveerd rond 14 °C

Ten gevolge van de gebruikte polymerisatie techniek blijven de ster polymeren hun chemische eindgroep behouden. De introductie van verschillende chemische eindgroepen zoals een azide en een amine was onderzocht op lineaire polymeren in het tweede deel van de thesis. De azide eind groep modificatie strategie was ook onderzocht op ster polymeren. In een preliminair experiment werd de bevestiging van poly(*p*-phenyleen vinyleen) polymeren aan deze azide eind groep gemodificeerde polymeren getest. In het laatste deel werd een kort drug opname experiment uitgevoerd waarin het potentieel van ster polymeren voor toekomstige 'drug delivery' experimenten werd onderzocht. Zelf-assemblage van de ster polymeren tot ultra-structurele complexen kan verwacht worden, hetgeen een positieve rol kan spelen in geval van drug opname.

De mogelijke temperatuurgevoelige eigenschap gecombineerd met de beloftevolle eerste indicaties over het drug opname potentieel stimuleert het uitvoeren van gedetailleerde studies met betrekking tot drug opname en gecontroleerde vrijzetting eens geoptimaliseerd. Daarenboven zal de correcte bevestiging van fluorescente PPVs het potentiële gebruik van ster polymeren voor (bio)beeldvorming toestaan. Het huidige werk heeft hierin dus een eerste stap gezet waarop verder onderzoek kan worden uitgebouwd.

1 Introduction

Ranging from plastic bottles to smartphone cases, polymers are one of the most widespread materials in everyday life. The sequential addition of monomers, to generate polymers is a powerful technique capable of forming a wide range of different and versatile materials.

Polymers are often formed by radical polymerization mechanisms employing radicals for monomer addition. Within this realm of radical polymerizations two major segments can be distinguished: Free radical polymerization (FRP) and reversible-deactivation radical polymerization (RDRP). The former expresses itself in a rather uncontrolled process during which radicals are produced thereby initiating the polymerization process. Radicals are generated by breakdown of an initiator molecule by heat, light or redox processes. The radical then attacks a monomer's carbon-carbon double bond forming a macroradical that can attack another monomer. This process called propagation, continues until the generating polymer chain is terminated. This occurs for example when the propagating chain couples with another (macro)radical or when the radical is transferred to another molecule (chain transfer). During FRP, initiation is constant until all initiator has been consumed or until the initiating stimulus is removed (e.g. heat). When initiation ends the FRP process comes to a complete stop and cannot be reactivated. In the end, broad molecular weight distributions are created which are constant with conversion.

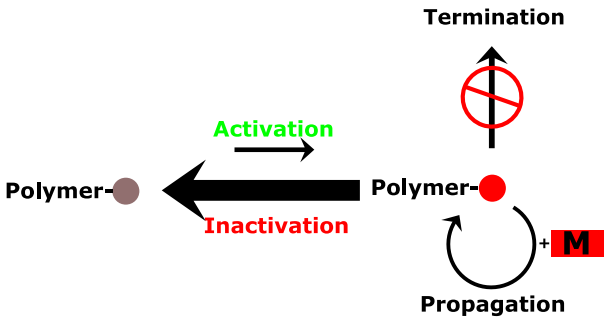

Figure 1: Schematic representation of the controlled radical polymerization principle. Favored reaction directions are represented by larger arrows.

RDRP techniques, on the contrary, are capable of forming polymers with precisely defined size and narrow molecular weight distributions. The RDRP process is based on three principles: rapid initiation, propagation reactions preferred over termination, and an equilibrium between active and dormant radical species favoring the dormant stage (Figure 1). As a consequence, the formed polymer chains all grow simultaneously and they maintain this growth behavior until completion. These polymers show therefore a linear growth with conversion, as opposed to this being constant in the case of free radical polymerization. Furthermore, polymerizations can be halted and restarted when desired.[1-2] This allows for the formation of well-defined polymer structures such as for example block copolymers. These are polymers composed out of different monomer types that are incorporated as well-defined segments.

Over the past two decades three main RDRP techniques have been discovered namely nitroxide mediated polymerization (NMP)[3], reversible addition-fragmentation chain transfer (RAFT)[4] and copper-mediated RDRP (CMP) such as atom transfer radical polymerization (ATRP)[5-7] and single electron transfer-living radical polymerization (SET-LRP)[8-9].

For CMP, the earlier described control is achieved by using copper(0) (Cu^0) or a copper-halogen complex, often copper(I)bromide (Cu^IBr) or copper(II)dibromide ($Cu^{II}Br_2$), together with a ligand molecule to aid solubilisation (Figure 2). The transition metal complex activates an alkyl halide (bromine end capped initiator or polymer), temporarily transferring the bromine from the polymer or initiator to the copper atom, forming $Cu^{II}Br_2$. This process brings the transition metal in a higher oxidation state and generates a radical allowing propagation to occur. However the propagating radicals are quickly deactivated by the $Cu^{II}Br_2$ complex forming once more Cu^IBr forcing the radicals back to the dormant state.[10]

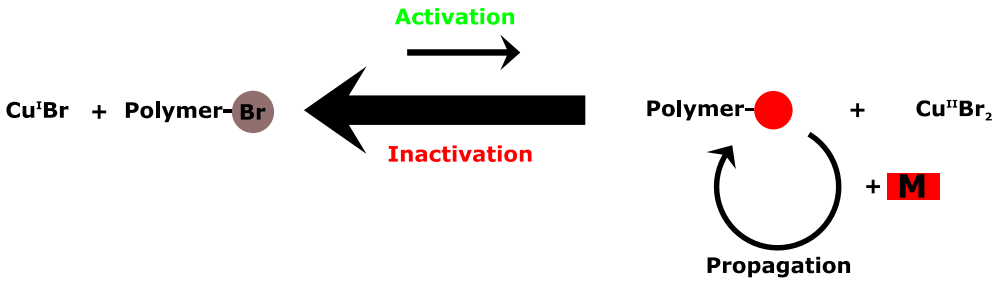

Figure 2: Schematic explanation of the general principle regarding copper-mediated controlled radical polymerization. Favored reaction directions are represented by larger arrows.

Recently it has been found that CMP can be initiated by employing light leading to the term photoCMP.[11-13] This way the on-off character of RDRP can be easily employed as if it were a simple light switch. This allowed researchers to perfectly fine-tune the sequential composition of polymers.[12,14] Furthermore, since light is theorized to regenerate the inactivated catalyst, the concentration of copper catalyst could be even brought down to ppm amounts, which is favorable when aiming for biological applications.[13,15]

The overall rise of RDRP enabled synthesis of a large variety of interesting materials. One of interest during this thesis is the star polymer. Star polymers are structures composed of a core molecule from which multiple polymeric chains, called arms, project outwards.[16] In general two approaches can be regarded when synthesizing star polymers: The "arm first"[17] and the "core first"[18] approach (Figure 3).

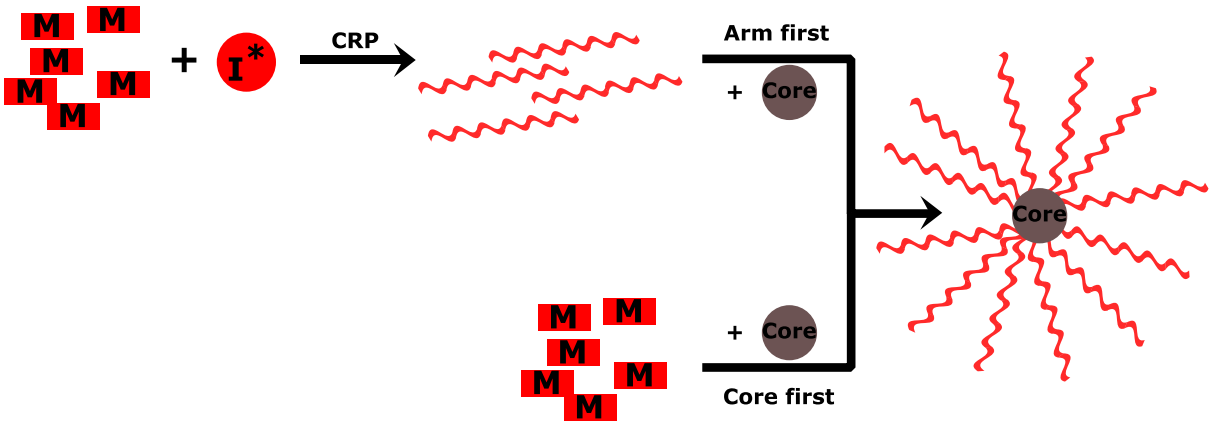

Figure 3: Two approaches exist to synthesize star polymers. Polymer chains are first synthesized via controlled radical polymerization techniques and afterwards attached to a core molecule in the arm first approach. In the core first approach, the polymer chains are directly grown from the core molecule.

Both techniques pose their own advantages and disadvantages. Preformed linear polymer arms (e.g. by RDRP techniques) are attached or crosslinked to a central core molecule in the arm first method. Efficient linkages between the core and polymer can be realized here for example via click chemistry.[17] While nicely defined arm lengths are achieved using this method, there is an uncertainty concerning the number of arms per star polymer in certain cases. This is overcome by utilizing multifunctional initiators used in the core first approach from which the arms are "grown" through state of the art RDRP techniques.[18-20] By using these techniques, the advantages of the known RDRP techniques such as uniform arm lengths and high end group fidelity also apply for star polymer synthesis.

Specialized materials such as star polymers are highly desired in the field of nanomedicine. This multidisciplinary field attempts to tackle major health problems such as cancer and Alzheimer's disease by using advanced nanoscaled materials to improve the efficiency of existing therapies. Despite many advancements in cancer therapy, quite brute approaches are still performed producing many unwanted side effects. This is caused by the broad effect of cytotoxic and cytostatic drugs also affecting a large fraction of healthy cells. These harmful drugs (often also hydrophobic) should ideally be shielded from healthy cells and only exposed to the targeted cancer cells in a controlled manner.[21] Several interesting examples were generated throughout time proposing solutions for this major health issue. Liposomes, double layered membrane structures, for example have a high stability in solution and are capable of encapsulating both hydrophobic as hydrophilic drugs. They have shown major progress and potential for drug delivery with already existing FDA approved commercial applications. However, upscaling of the synthesis process is rather tedious since there is a lack of large scale reproducible synthesis methods. Moreover, there commonly is only limited control over the drug release.[22]

Micelles, on the other hand, are self-assembled structures of surfactant molecules capable of encapsulating hydrophobic drugs in their inner hydrophobic environment.[23] Control over the release of the cargo has been demonstrated as

well.[24-25] Despite their interesting and promising properties a major drawback is their lack of stability. Micelle stability is concentration dependent meaning that they only form above a certain concentration denoted as the critical micelle concentration (CMC). When administered in the human body this concentration can rapidly drop leading to breakdown of the structures and a burst release of their cargo which is of course highly undesired.[26] Star polymers consist out of only one molecule and are therefore sporadically addressed as unimolecular micelles.[27] In the end these polymers pose micellar-like properties but do not suffer from the necessity of a certain CMC.[16] Star polymers possess several more advantages proving their splendid versatility and potential as future nanotherapeutic material (Figure 4).

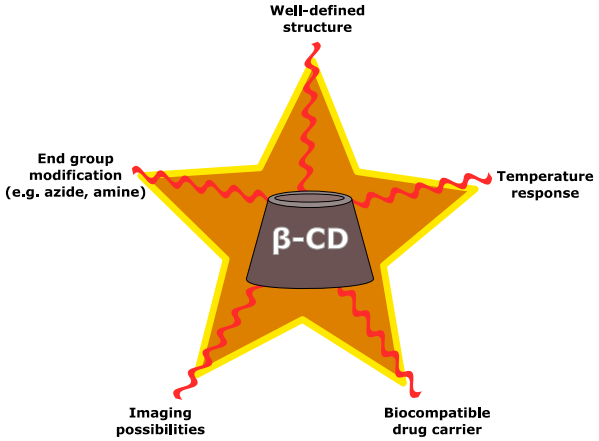

Figure 4: Versatile potential of star polymers composed of a β-cyclodextrin core in biomedical applications.

A tunable thermo-responsive behavior can be easily implemented in star polymers by selecting specific building blocks which are known to change properties upon a variation in temperature. This temperature response is often reversible occurring around a certain temperature known as the lower critical solution temperature (LCST), where the polymer becomes soluble below this temperature. When the polymer becomes soluble above a certain temperature this temperature point is called the upper critical solution temperature (UCST).[28] Thus, advanced star-shaped polymers that can respond to a change in the biological environment (e.g. by agglomeration) can be synthesized. This stimuli-responsive character can be used further to control drug release improving the therapeutic efficiency of existing drugs.[29-30] Furthermore, each star polymer contains a high density of chemical groups on its surface and along the arms.[16] These can be modified enabling for example click chemistry, drug conjugation and bio-imaging. Rendering the star polymer biocompatible is also of major interest since all nanomaterials – including the star polymer - are rapidly covered by proteins when presented in the human body. This so called protein corona affects the final fate of the particle as well as its biological identity.[31] Nevertheless formation of the protein corona can be minimized by modifying the particle's surface with antifouling structures such as poly(ethylene glycol) which is shown to increase the circulation time of the particle.[32] Studying the protein corona formation on star polymers as well as the prevention thereof is not the purpose of the current work. Nevertheless

implementation of poly(ethylene glycol) brushes in the arm structure of the star polymer as block functionalities can be envisioned when RDRP techniques are used enabling future testing of this antifouling property.[20]

Well-defined structures concerning size, size distribution and number of arms are very important when aiming for biological applications. A high amount of control can be achieved when RDRP techniques in the core-first method are employed. An interesting core structure known as β-cyclodextrin (β-CD, Figure 4) provides an ideal starting point. This supramolecular structure is a 7-membered sugar ring that can be modified into a (photo)CMP initiator containing up to 21 initiating groups. Hence, up to 21-arms can be synthesized with high precision.[18,20] Furthermore, it was also demonstrated that this molecule can be modified selectively providing different functional-groups to allow Janus particle synthesis.[33]

Starting from existing work in our labs regarding synthesis of 21 arm star polymers, the concept was further elaborated. The central purpose of this project was the synthesis of multifunctional thermo-responsive star polymers. The intended chemical moieties to be attached to the star shaped polymers are: an azide molecule (N_3) for click chemistry and an amine molecule (NH_2) to explore direct peptide synthesis exploiting the thermo-responsive property. Imaging and drug delivery as potential biomedical applications will be examined in the final phase as a proof of principle. To summarize, this thesis will further explore how and for which purposes star polymer structures can be applied in the field of nanomedicine. The research will contribute to the beginning phase of the fundamental development and understanding of these smart materials. This will pave the way on which future steps towards state of the art applications such as controlled drug delivery and imaging will be taken once optimized synthesis procedures are established. This approach will definitely lead to a major improvement in the outcome of for example cancer therapies.

2 Materials and Methods

2.1 Materials

All common solvents and salts were bought from Acros Organics, Fisher Chemical, or VWR Prolabo Chemicals and used as delivered. The following reagents and catalysts were purchased and used without further purification: copper(I)bromide ($Cu^{I}Br$, Acros Organics, 98%), copper(II)dibromide ($Cu^{II}Br_2$, 99%, Sigma-Aldrich), *N,N,N′,N′′,N′′*-Pentamethyldiethylenetriamine (PMDETA, 99%, Acros Organics), 2-bromoisobutyryl bromide (97%, Alfa Aesar), Ethyl α-bromoisobutyrate (EBiB, >98%, Alfa Aesar), β-cyclodextrin (β-CD, 98%, Acros Organics), sodium azide (NaN_3, >99.5%, Sigma-Aldrich), palladium on activated charcoal (Pd/C, 10 wt%, Janssen Chimica), triphenylphosphine (PPh_3, 99%, Fisher Chemical), phtalimide potassium salt (99%, Acros Organics), potassium hydroxide (KOH, >85%, Fischer Chemical), triethylamine (TEA, 99%, Acros Organics) and hydrazine monohydrate (98%, Sigma-Aldrich). Methyl acrylate (MA, 99%) and di(ethylene glycol) ethyl ether acrylate (DEGA, >98%) were purchased from Acros Organics and TCI Europe and deinhibited over a column of basic alumina before use. Rhodamine B dodecyl ester (>95%) was acquired from Sigma Aldrich. Tris-(2(dimethylamino)ethyl)amine (Me_6TREN)[34], *N*-Boc-propargylamine[35] and poly[2-methoxy-5-(3′,7′-dimethyloctyloxy)-1,4-phenylene-vinylene] (MDMO-PPV) blocks with alkyne functionalities[36] were synthesized following literature procedures.

2.2 Analysis

Proton-Nuclear Magnetic Resonance (^{1}H-NMR) All NMR samples were measured in deuterated chloroform ($CDCl_3$). Measurements were performed on a 400 MHz NMR spectrometer (Oxford Instruments Ltd.) with 64 scans and an applied 12 second pulse delay between scans using a Varian probe (9 mm 4-nucleus Auto-SWPFG).

Gel Permeation Chromatography (GPC) Polymer size distributions were measured using a Tosoh EcoSEC HLC-8320GPC consisting out of an autosampler and a PSS guard column SDV (50 × 7.5 mm), followed by three PSS SDV analytical linear XL columns (5 μm, 300 × 7.5 mm) and a differential refractive index detector (Tosoh EcoSEC RI). Column temperature was maintained at a constant 40 °C and the column molecular weight range goes from 1×10^2 to 1×10^6 g·mol^{-1}. A flow rate of 1 mL·min^{-1} of high-performance liquid chromatography (HPLC) grade tetrahydrofuran (THF) was used as eluent with toluene as flow marker. Calibration was performed using linear narrow polystyrene (PS) standards from PSS Laboratories in the range of 470-7.5 × 10^6 g·mol^{-1}. MHKS parameters for poly(methyl acrylate) (pMA) (α = 0.74, K = 10.2 × 10^{-5} dL·g^{-1}, THF 30 °C)[37] were used for sample analysis.

Electrospray Ionization Mass Spectrometry (ESI-MS) Spectral mass analysis was performed using an LCQ Fleet mass spectrometer (ThermoFischer Scientific) equipped with an atmospheric pressure ionization source set in nebulizer assisted electro spray mode. Calibration was performed in the mass/charge (m/z) range of 220–2000 with a standard solution containing caffeine, L-methionyl-arginyol-phenylalanylalanine acetate H_2O and Ultramark 1621. A constant spray voltage of 5 kV was employed with an applied nitrogen dimensionless auxiliary gas flow-rate of 3 and a dimensionless sheath gas flow-rate of 3. The capillary voltage, tube lens offset voltage and capillary temperature were set to 25, 120 V, and 275 °C, respectively. A 250 μL aliquot of a polymer solution with concentration of 10 $\mu g \cdot mL^{-1}$ was injected with HPLC grade THF and methanol (THF:methanol 3:2) as solvent.

Transmittance measurements Transmittance at various temperatures was recorded from 480 nm to 520 nm using a Cary 5000 ultraviolet-visible light (UV-VIS) spectrophotometer (Agilent Technologies).

Plate reader Absorbance spectra were recorded from 220 nm to 500 nm from top to bottom using a FLUOstar OMEGA Microplate Reader (BMG Labtech GmbH). Fluorescence measurements were performed by exciting fluorescent molecules at 544 nm using a gain of 750 and recording the emission at 590 nm, unless stated otherwise. 20 flashes per well were set for both measurements.

Dynamic light scattering (DLS) Particle size distributions were measured using a Brookhaven Instruments ZetaPALS for a 0.1 wt% star polymer solution in H_2O.

2.3 Methods

21-arm initiator synthesis (21BrCD) 21BrCD was synthesized starting from β-CD using a combination of two literature procedures.[18,38] β-CD (5.7 g, 5.022 mmol, 1 eq.) and triethylamine (30.7 mL, 220.97 mmol, 44 eq.) were dissolved in a 250 mL three-neck round-bottom flask with 100 mL THF. The solution was stirred in an ice bath for 10 minutes and purged with argon. 2-bromoisobutyryl bromide (27.3 mL, 220.97 mmol, 44 eq.) dissolved in 40 mL THF was added slowly. The solution was allowed to return to room temperature overnight under continued stirring. Next, the solution was transferred to a separatory funnel with 300 mL diethyl ether and extracted once with 200 mL H_2O, three times with 200 mL saturated sodium bicarbonate ($NaHCO_3$) solution and a final time with H_2O. The organic phase was dried over magnesium sulfate ($MgSO_4$), filtered and the solvent was removed by rotary evaporation until a brown oil was obtained. The oil was then precipitated in an excess of *n*-hexane and the formed crystals were filtered of by vacuum filtration. ^{1}H-NMR ($CDCl_3$, 400 MHz, δ): 1.81 (s Br, 126H, CH_3), 3.5-5.4 (49H, sugar residues).

When purified initiator is used, the crystals were afterwards purified over a silica column with toluene and ethyl acetate in a 3:1 ratio as eluent. The initiator fraction was concentrated by rotary evaporation to yield a yellow oil that was then

precipitated in an excess of *n*-hexane. The solution was finally filtered by vacuum filtration yielding white crystals.

General batch polymerization procedure 21BrCD (macro)initiator, $Cu^{II}Br_2$ (0.010 eq. per CH-Br), Me_6TREN (0.075 eq. per CH-Br) and MA or DEGA were added to an amber volumetric flask (differing eq. depending on desired arm/block length) and the reaction mixture was diluted with dimethyl sulfoxide (DMSO). The homogenous solution, obtained after ultrasonication, was then transferred to a transparant Erlenmeyer flask. Next, the solution was shielded from light and purged with nitrogen for 15 to 45 minutes - depending on the reaction volume. The polymerization was started by placing the solution in a Multilamp Reactor MLU 18 (Photochemical Reactor Ltd.) equipped with ten 15 Watt lamps (Vilber Lourmat) having a peak emission of 365 nm. Afterwards, the polymer solution was extracted twice with 25 mL of chloroform (and a large excess of H_2O. The organic phase was then washed twice with plenty of water before removing the solvent by rotary evaporation. Finally, the polymer mixture was filtered over a short silica column with THF and placed overnight in a vacuum oven for drying.

General flow polymerization procedure 21BrCD or ethyl α-bromoisobutyrate (EBiB, >98%), $Cu^{II}Br_2$ (0.010 eq. per CH-Br), Me_6TREN (0.075 eq. per CH-Br) and MA or DEGA (differing eq. per CH-Br depending on desired arm length) were added to two different amber volumetric flasks and diluted with DMSO. Premature polymerization was prevented by separating the monomers from the rest of the reaction mixture. The homogenous solutions, obtained after ultrasonication, were shielded from light and purged with nitrogen for 7 to 30 minutes – depending on the volume of the reaction mixtures. The mixtures were then transferred to two degassed syringes (HSW® Norm-Ject® Sterile Luer-Lock) of appropriate volume. Polymerizations were carried out either in a 2 mL glass chip reactor (Uniqsis flow reactor, Uniqsis Ltd) placed in an ultraviolet (UV) nail curing lamp (VidaXL, λ_{max} = 365 nm) or in transparent perfluoroalkoxy tubing (PFA, inner diameter = 0.75 mm, APT advanced polymer tubing GmbH) wrapped around a 15 Watt UV lamp (λ_{max} = 365 nm, Vilber Lourmat). Mixing of the reaction mixture occurs automatically in the glass chip reactor, while a static mixing unit (Upchurch Scientific) was incorporated in the latter set-up. A syringe pump (Fusion 200 Chemyx Syringe Pump, Chemyx Inc) was used to control the flow speed for both set-ups. Samples were taken at various residence times to allow screening of the reaction.

General procedure for the generation of an azide end group The azide end group was introduced in the (star)polymers using known literature procedures for linear polymers.[39] (21-arm star)polymer and sodium azide (NaN_3, >99.5%, 2 eq. per CH-Br) were stirred for 5 hours at room temperature in 40 mL *N,N*-Dimethylformamide (DMF). The solution was transferred to a separatory funnel with 50 mL diethyl ether and extracted 3 times with 50 mL H_2O. The organic phase was dried over $MgSO_4$ and the solvent was removed by rotary evaporation.

Copper(I)-catalyzed alkyne-azide cycloaddition (Cu^{I}AAC) of azide end group modified (star)polymers with *N*-Boc-propargylamine Cu^{I}AAC was performed using known literature procedures for linear polymers.[40] Azide end group modified (star)polymers and *N*-Boc-propargylamine (2 eq. per CH-N_3) were weighed out in a vial and dissolved in 1 mL DMF. Next, Cu^{I}Br (2 eq. per polymer) and *N,N,N′,N′′,N′′*-Pentamethyldiethylenetriamine (PMDETA, 99%, 4 eq. per polymer) were weighed out in a separate vial and dissolved in 1 mL DMF. The two mixtures were degassed, mixed and stirred overnight at room temperature inside a glovebox. After adding 15 mL H_2O the solution was extracted twice with 2 mL CH_2Cl_3. Finally, the solvent was removed by rotary evaporation and the mixture was filtered over a short silica column with THF.

Afterwards, the *tert*-butyloxycarbonyl (Boc) protecting group was cleaved off by following a literature procedure[41] yielding a primary amine end group.

Copper(I)-catalyzed alkyne-azide cycloaddition (Cu^{I}AAC) of azide modified star polymers with alkyne functionalized MDMO-PPV polymers The alkyne functionality of the MDMO-PPV polymer (M_n = 8 200 g·mol^{-1}, $Đ$ = 1.43) was deprotected before Cu^{I}AAC by following a literature procedure.[36] A 5 mL solution of azide end group modified star polymers (0.1 g, 0.197 μmol, 1 eq., M_n = 507 200 g·mol^{-1}, $Đ$ = 1.18) and MDMO-PPV block with alkyne functionality (0.037 g, 4.55 μmol, 1.1 eq. per CH-N_3) was mixed with Cu^{I}Br (0.1 mg,0.986 μmol, 5 eq.) and PMDETA (0.2 mg, 0.986 μmol, 5 eq.). The reaction mixture was purged with nitrogen for 15 minutes and stirred for 1 week. 10 mL of water was added and the solution was extracted twice with 5 mL CH_2Cl_3. The solvent was removed by rotary evaporation while shielding the mixture from light.

Cooled H_2O (4 °C) was added to the crude polymer mixture and kept at 0°C for 30 minutes. Afterwards the solution was filtered and the filtrate was lyophilized overnight to yield a mixture of clicked and unclicked star polymers.

General procedure for the generation of an amine by catalytic reduction of the azide end group Azide end group modified polymer (M_n = 1 600 g·mol^{-1}, $Đ$ = 1.12) and a spatula tip of Pd/C were added to a three neck flask fitted with a glass stopper, a valve and a septum. The polymer was dissolved in a 50:50 mixture of ethanol and ethyl acetate and stirred while purging with nitrogen for 15 minutes. Afterwards the solution was purged with hydrogen for 15 minutes before applying a constant hydrogen atmosphere through the valve. The solution was stirred overnight and afterwards filtered over Celite® with CH_2Cl_3. Finally, the solvent was removed by rotary evaporation.

General procedure for the generation of an amine end group via the Staudinger reaction[39] Azide end group modified polymers and triphenylphosphine (PPh_3, 99%, 1.20 eq. per CH-Br) were dissolved in 20 mL THF and stirred overnight at room temperature. Afterwards, *n*-hexane was added and the precipitate was filtered off. The filtrate was concentrated *in vacuo* and afterwards dissolved in 5 mL THF. 100 mL H_2O was added and the solution was

stirred for two days at room temperature. Next, *n*-hexane was added and the precipitate was filtered off. Finally, solvents were removed from the filtrate by rotary evaporation.

Generation of an amine end group via the Gabriel Synthesis[42-43] Linear polymers (with bromine end group, 1.520 g, 1 mmol, 1 eq.) and phtalimide potassium salt (99%, 0.213 g, 1.1 mmol, 1.1 eq.) were dissolved in DMF and refluxed for 3 hours at 154 °C. There are two option to cleave the phtalimide end group. Either by (1) hydrolysis with potassium hydroxide (KOH) or (2) by hydrazinolysis using hydrazine monohydrate (98%). In the first method, the phtalimide end group modified polymers were mixed with KOH (0.16 g, 2.8 mmol, 10 eq.) and refluxed in 10 mL *tert*-butanol overnight at 80 °C. Afterwards, the solvent was evaporated and 10 mL H_2O was added. The aqueous phase was then acidified to pH 2 using hydrogen chloride (HCl, 1M) and extracted three times with 5 mL dichloromethane (DCM), yielding amine end group modified polymers after removing the solvent by rotary evaporation. In the second method, the phtalimide end group modified polymers were dissolved in 15 mL THF and mixed with hydrazine monohydrate (0.0751 g, 1.5 mmol, 5 eq.) dissolved in 5 mL methanol. This solution was refluxed for 24 hours at 55 °C. Finally, 5 mL saturated sodium hydroxide (NaOH) solution was added and the aqueous phase was extracted twice with 5 mL CH_2Cl_3 yielding amine end group modified polymers after removal of the solvent by rotary evaporation.

Thermo-responsive experiments Thermo-responsive 21 arm diblock copolymers were dissolved in cold water (0.5 wt%, see Table 2 for specifics). Cold samples (0-5 °C) were transferred to small reaction tubes and fitted in a UV-VIS spectrophotometer. Samples were stirred and allowed to heath up slowly on their own accord. Temperatures were constantly measured and at each degree incline a transmittance spectrum was recorded from 480 nm to 520 nm.

Loading with a fluorescent dye (rhodamine B dodecyl ester) Thermo-responsive 21 arm diblock copolymers (M_n = 590 600 g·mol^{-1}, $Đ$ = 1.15) were dissolved in H_2O (0.1 wt%). And transferred to a vial before adding 10 ppm rhodamine B dodecyl ester. The vial was stirred for 30 minutes in an icebath and afterwards quickly heated up and centrifuged for 15 minutes at 4 300 rpm. The supernatants was removed and the pellet weighed out before dissolving in 2.5 mL ethanol to release the fluorescent dye. The solution was distributed over a 96 well plate (Greiner® UV Star® Flat-bottom) plating 3 wells per condition with 200 μL per well. The amount of rhodamine B dodecyl ester was calculated afterwards via a standard curve.

3 Results and Discussion

3.1 Star polymer synthesis

3.1.1 Usage of photoflow reactors for star polymer synthesis

The described photoCMP mechanism was used to synthesize star polymers. This can be achieved using batch reactors as well as continuous (photo)flow reactors, as demonstrated by Wenn et al.[20] By switching from a batch oriented synthesis of polymers to a continuous flow approach, the efficiency of the reaction can be drastically optimized minimizing batch-to-batch variations and maintaining rather mild reaction conditions (e.g. lower light intensity).[44] Aside from the use of flow for safe, fast and economic screening of reactions, it is also increasingly used for upscaling and exploring dangerous or forbidden chemistry. Especially regarding scaling up of reactions, the use of flow for light initiated polymerizations is highly advantageous. Batch reactors usually possess a significant inactivated volume through which light is unable to penetrate as a consequence of Lambert-Beer's law. In photoflow, this limitation is overcome since the used reactors have a diameter of only a few millimeters which leads to more efficient irradiation of the reaction mixture.[44] This can speed up the reaction from days to even minutes in certain cases. The amount of degradation products is also reduced since lower light intensities can be used and the total illumination time is reduced compared with batch.[45-46] Moreover, several regulating authorities such as the food and drug administration (FDA) stimulate the use of continuous flow for active pharmaceutical ingredient development.[47] For these reasons the decision was made to further develop the use of photoflow to synthesize the 21-arm star polymers. Synthesis of this specific polymer was already performed as a proof of principle during previous studies by Wenn et al, mainly using batch procedures.[20]

3.1.2 Molecular weight analysis of star polymers

Gel permeation chromatography (GPC) measures the molecular weight of polymers by passing the polymer mixture through a column packed with porous material. This column separates polymers by hydrodynamic volume. As a rule of thumb it is stated that short polymer chains with a small hydrodynamic volume will pass slower through the column compared with bigger polymers that have a larger hydrodynamic volume. The molecular weight of the measured polymer can then be calculated via application of polymer specific variables (Mark Houwink parameters) based on polystyrene calibration. Therefore it should be remarked that molecular weight analysis of star polymers by GPC is a rather rough estimation since calibration of the device is performed using linear standards in contrast with the branched or star structures synthesized during this thesis. Nevertheless a literature known factor can be used to correct the measured molecular weight by GPC to a certain extent.[48] A comparison between measured, corrected and theoretical molecular weight values can be found in SI 1 (a). Furthermore a

comparison is also given for a reaction performed on an initiator capable of growing 4 arms (SI 1, b).[20] It can be seen that this correction factor gives an accurate approximation of the molecular weight of 4-arm star polymers. This approximation is however less accurate for 21-arm star polymers, most likely since this factor applies for polystyrene star polymers that were synthesized with the 'arm first' method and do not contain a β-CD core as is the case for the star polymers in the current work. Therefore more accurate correction factors or the use of precise techniques to determine the molecular weight such as static laser scanning or on-line viscosity monitoring as suggested by Radke et al should be envisioned.[48] The use of static laser scanning was nicely demonstrated by Haddleton et al, obtaining measured molecular weight values of 21-arm poly(methyl methacrylate) star polymers close to the theoretical molecular weight obtained from monomer conversion measured by ^{1}H-NMR.[18] This approach was unfortunately not possible during this thesis since the necessary instrument was not part of the available in-house measurement techniques.

3.1.3 Synthesis of star polymers with short arms

As a first experiment a star polymer was synthesized with a targeted arm length of 2 000 g·mol^{-1} of methyl acrylate (MA), which is considered relatively short. A homemade flow reactor consisting out of perfluoroalkoxy (PFA) tubing and a UV lamp with a volume of 2 mL was used. Figure 5 shows the first order plot (Figure 5, a) and GPC traces (Figure 5, b) for this performed reaction.

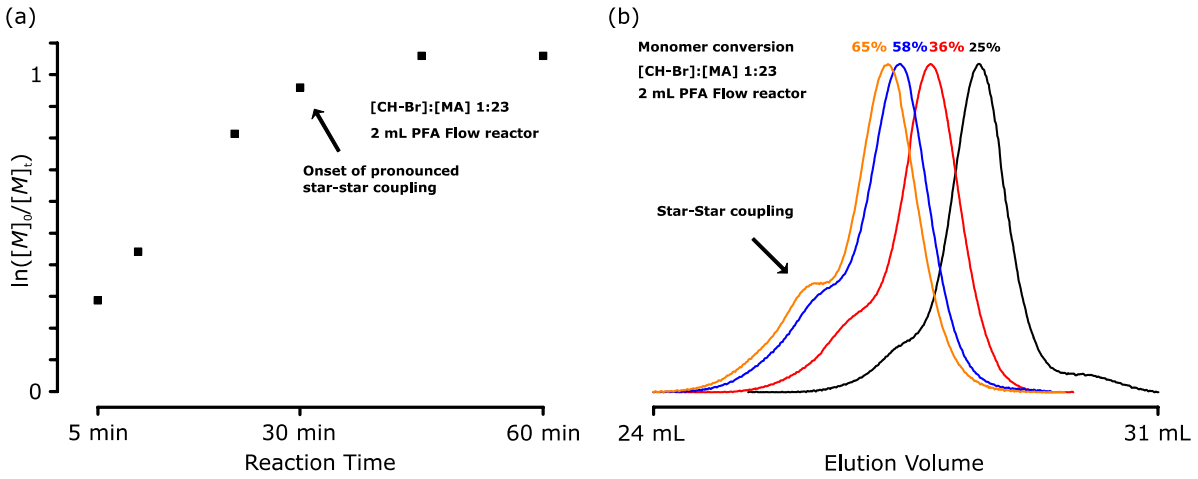

Figure 5: Reaction monitoring of methyl acrylate polymerization in the homemade 2 mL PFA flow reactor. The plot of ln($[M]_0/[M]_t$ over time (a) for star polymers with a targeted arm length of 2 000 g·mol^{-1} as well as its GPC traces (b) are given. Star-star coupling is marked with an arrow. The [CH-Br]:[$Cu^{II}Br_2$]:[Me_6TREN]:[MA] equivalents used were 1:0.01:0.075:23 with a monomer to solvent (DMSO) dilution of 1:30.

A controlled character of the polymerization can be observed up till reaction times of 30 minutes. This is reflected by a linear distribution of the time points up till 30 minutes in the first order plot (Figure 5, a). In GPC shifts of the star polymer distribution to lower elution volumes for increasing conversion are observed (Figure 5, b). This reflects the increase in molecular weight for increasing conversion which also demonstrates the controlled character of the polymerization. However, after 30 minutes this linear distribution levels off possibly indicating

termination events or loss of functional end groups. For star polymers this is most likely due to star-star coupling. This process occurs with a certain probability when propagating radicals of growing arms from neighboring polymers meet and couple – which is in fact an intermolecular termination event. This coupling process can be observed as well by a high molecular weight shoulder presented in the GPC traces which increases when higher conversions are reached (Figure 5, b, arrow). The appearance of this shoulder can be explained by the fact that when two growing star polymers couple the molecular weight doubles. Therefore an additional polymer distribution (with a higher molecular weight) emerges in the GPC traces.

Star-star coupling is a known effect among star polymer synthesis, being observed as well for different star polymers previously synthesized by Wenn et al.[20] The coupling process was also observed for 21-arm star polymers synthesized in batch by other groups using a similar core initiator structure.[18,49]

3.1.4 Reduction of star-star coupling

In general there are two approaches to minimize the intermolecular termination event which leads to star-star coupling. First, one can dilute the reaction mixture.[18,20] However, in the above polymerization (Figure 5) already a rather high dilution is used (monomer to solvent ratio of 1:30). Diluting higher would slow down the reaction drastically which in the end removes an important advantage of photoflow. Secondly, the reaction can be halted when 50-60% conversion is reached, before significant coupling starts to emerge.[20,49] Removal of solvent (DMSO) can be tedious and costly compared with the removal of unreacted monomers, therefore the latter solution is often preferred. As an alternative, Matyjaszewski recently reported the synthesis of β-CD based star polymers via electrochemically mediated CMP of *n*-butyl acrylate.[50] Termination events (both inter- and intramolecular) were suppressed by applying a less negative potential. This effectively minimized the amount of star-star coupling. Yet, despite showing narrow size distributions, the reactions still took quite long and a higher ppm of Cu^{II} species is used compared with the polymerizations performed in the present thesis. Therefore the advantages of using photoCMP still stand.

3.1.5 Synthesis of star polymers with long arms

For future aimed star polymer applications (e.g. drug loading), longer arms are desired since this will lead to a larger macromolecule which can hold an increased amount of hydrophobic drug. Overall, literature reports on rather short arm lengths comparable with previous work on different star shaped polymers by Wenn et al (regardless of the mechanism and used monomers).[18,20,33,49,51] Only Haddleton and coworkers recently reported the synthesis of 8-arm star polymers with theoretical arm lengths up to 16 000 $g \cdot mol^{-1}$.[19] These experiments were however performed in batch and reactions were ran overnight.

To achieve the future goal of increased drug loading a higher arm length up to 10 000 g·mol^{-1} was targeted. In Table 1 the results for polymerizations performed for different reaction conditions and reaction set-ups are summarized. What was observed was that for polymerizations performed in the homemade 2 mL PFA flow reactor minimal to no reaction occurred (0% conversion, Table 1). To investigate whether this result was due to the reactor set-up, a similar reaction was performed in a commercial 2 mL glass chip flow reactor (Uniqsis) using a UV nail curing lamp as UV source, similar to the work of Haddleton and coworkers on linear polymers.[12,52]

Table 1: Comparison of conversion and molecular weight (M_n) of the polymers synthesized in the homemade 2 mL PFA flow, the 2 mL glass chip and the batch reactor. Arm lengths were targeted for 10 000 g·mol^{-1}. The [CH-Br]:[Cu^{II}Br$_2$]:[Me$_6$TREN]:[MA] equivalents used were 1:0.01:0.075:116. DMSO was used as solvent.

Reactor	Reaction time (minutes)	Monomer:solvent dilution	Monomer conversion (%)	$M_{n,\ theoretical\ total\ star}$ [a] (g·mol^{-1})	$M_{n,\ corrected\ total\ star}$ [b] (g·mol^{-1})	$Đ_{,\ total\ star}$
2 mL PFA Flow	20	1:35	0	-	-	-
Glass Chip Flow	20	1:35	13	32 000	30 000	1.19
Glass Chip Flow	60	1:35	36	80 000	84 000	1.15
Glass Chip Flow	20	1:15	33	74 000	82 000	1.15
Batch	60	1:40	26	59 000	49 000	1.12
Batch	60	1:15	44	97 000	140 000	1.11

[a] Calculated via conversion. [b] M_n measured by GPC and corrected with a factor (2.73) taken from literature[48].

It appeared that the glass chip flow reactor provided better reaction conditions compared with the PFA reactor for identical reaction times (20 minutes, 13% conversion, glass chip flow reactor, Table 1). Furthermore, an increase in conversion was observed for the glass chip flow reactor for longer reaction times while maintaining rather low dispersities (60 minutes, 36% conversion, $Đ$ = 1.15, Table 1). Shoulder formation was absent in these conditions as well even for reaction times up to two hours as shown in the GPC traces in Figure 6.

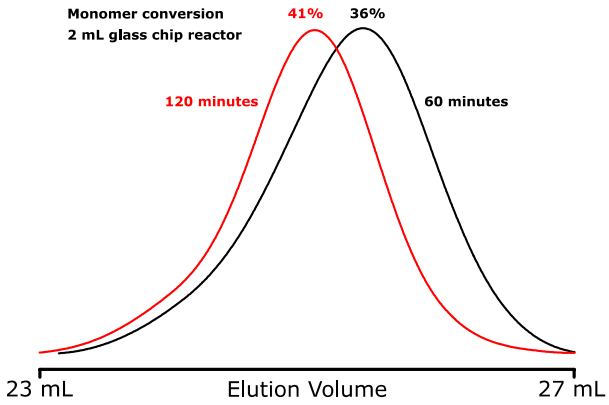

Figure 6: Effect of increased reaction time for polymerization performed in the 2 mL glass chip flow reactor. Arm lengths were targeted for 10 000 g·mol^{-1}, [CH-Br]:[Cu^{II}Br$_2$]:[Me$_6$TREN]:[MA] equivalents used were 1:0.01:0.075:116 with a monomer to solvent (DMSO) dilution of 1:35.

This desired polymerization behavior indicates that star polymer synthesis via continuous flow approaches is possible. However, the reaction occurs in rather dilute conditions (monomer to solvent dilution of 1:35) and requires long reaction

times (up to 2 hours, 41% conversion, Figure 6). Therefore it was investigated whether concentrating the reaction mixture (lower monomer to solvent dilutions) further improves the reaction. In this regard, higher conversions were reached in batch when the reaction mixture was concentrated (monomer:solvent dilution of 1:15, 44% conversion, Table 1 and SI 2). Additionally, increased conversion was already observed after only 20 minutes in the glass chip reactor (33% conversion, monomer:solvent dilution of 1:15, Table 1) stating the advantage of continuous flow techniques.

3.1.6 Synthesis of star polymers with long arms after initiator purification

Despite the favorable results from star polymers synthesized in the glass chip flow reactor, this set-up does not allow for much upscaling due to the limited reactor volume (fixed at 2 mL). As was indicated by the results in Table 1 more concentrated reaction mixtures would be desired to allow efficient reactions to occur. Furthermore a hypothesis was given that the previously shown problems might also be due to unpure 21-arm initiator. Therefore, a protocol was followed to remove any present impurities via column chromatography.[18]

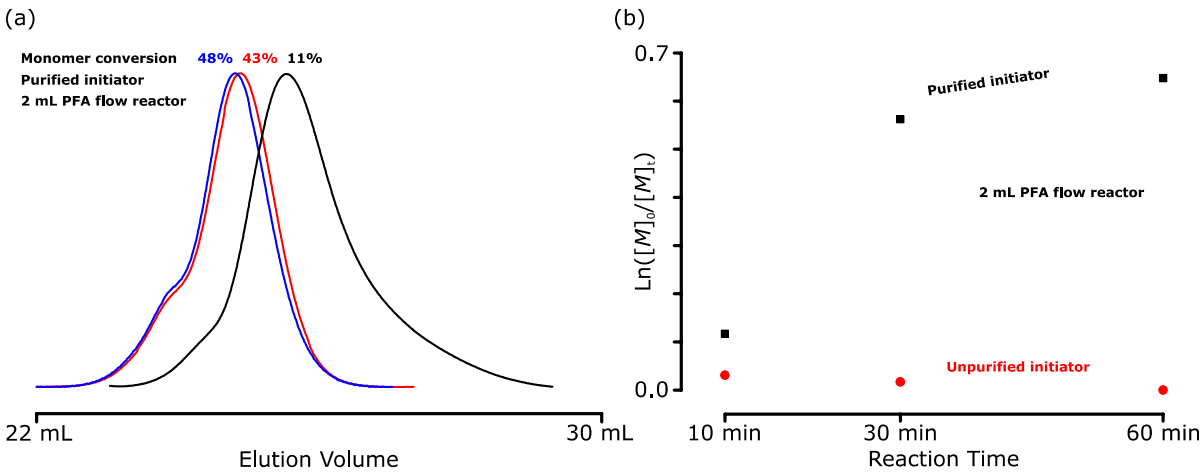

Figure 7: The effect of performing 21-arm initiator purification via column chromatography for polymerizations performed in the homemade 2 mL PFA flow reactor. GPC traces of the reaction performed with purified initiator (a) and the first order plot comparing reactions performed with purified (b, ■) and unpurified (b, ●) initiator are given. Arm lengths were targeted for 12 000 g·mol^{-1}, [CH-Br]:[Cu^{II}Br$_2$]:[Me$_6$TREN]:[MA] equivalents used were 1:0.01:0.075:139 with a monomer to solvent (DMSO) ratio of 1:30 for the reaction with unpurified initiator and 1:10 for the purified one.

The GPC traces as well as the first order plot for polymerizations with a high targeted arm length are given are shown in Figure 7. The first order plot of a comparable reaction performed with unpurified initiator was also included.

Despite the observed star-star coupling, a controlled behavior can once more be detected in (Figure 7) reaching a monomer conversion of 48% after one hour. This result is positive, yet strange since impurities in the initiator mixture never presented any deleterious effects on the polymerization of star polymers with short arm lengths (Figure 5). In addition, differences between batch reactions with pure and unpure reactions were minimal suggesting that flow polymerization is more susceptible to impurities in the reaction mixture. Nevertheless, for future studies 21-arm initiator synthesis should be further optimized to prevent the presence of

impurities as much as possible since this appears to have an immense effect on polymerization efficiency. An improvement could lie in the use of a different solvent as reaction medium. In literature the use of *N*-methyl-2-pyrrolidone is suggested, improving the dissolution of the β-CD starting product.[38,53]

The findings in this part led to a more optimized synthesis of 21-arm star polymers using continuous flow techniques. This optimization procedure was tedious and requires further investigation to allow full understanding of the reaction mechanism. This will help to switch from batch to continuous flow procedures to allow convenient upscaling of the polymerization process.

3.2 Star block copolymerization

Several groups have reported on the diblock synthesis of 21-arm star polymers using controlled radical polymerization techniques to introduce temperature-responsive properties.[49,51] Implementing a certain stimuli-responsive property enables the exploration of biomedical applications such as drug delivery. Furthermore diblock synthesis of the arms even allows the star polymer to form complex structures such as micelles.[20,33]

3.2.1 Introduction of thermo-responsive di(ethylene glycol) ethyl ether acrylate monomers

Most work on thermo-responsive polymers has been performed on poly(N-isopropylacrylamide) (pNIPAM). This structure is often regarded as ideal for biological applications due to its LCST being fixed around 32 °C in water independent of the chemical environment.[28] Capable competitors of this established structure are short oligo(ethylene glycol) (meth)acrylate polymers. These polymers can be copolymerized with other monomers to tune the LCST which is usually not possible in the case of pNIPAM. Another major advantage of using these branched materials for the synthesis of nanoscaled materials for bioapplications is the known protein repellant effect of poly ethylene glycol (PEG). This leads to lower immune responses and improved circulation times of the particle due to minimized protein corona formation. Therefore PEG is often used in antifouling surfaces, tissue engineering and of course drug delivery.[54]

For this thesis the choice was made to perform block copolymerization of MA together with di(ethylene glycol)ethyl ether acrylate (DEGA) as shown in Figure 8. Using MA as inner block and DEGA as outer 'shell', a large hydrophobic inner structure is created with a reversible hydrophobic-hydrophilic mantle depending on the surrounding temperature. Synthesis of these star polymers was performed in batch since these experiments were performed before the problems in flow were identified.

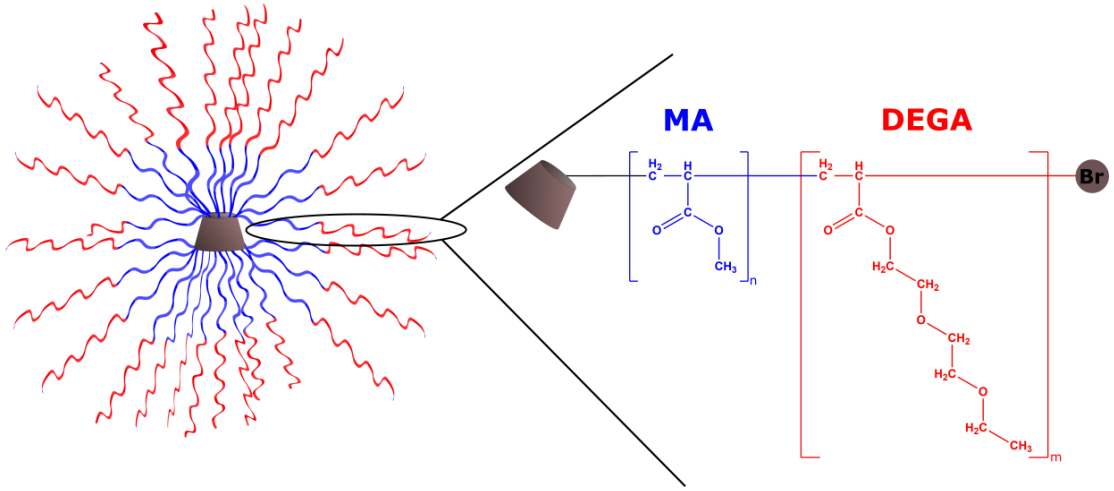

Figure 8: Schematic representation of the aimed block copolymerization of 21-arm star polymers with MA (as inner core) and DEGA (as shell). Note that the bromine end group is maintained after controlled polymerization.

Figure 9 shows a typical GPC trace which was observed for all synthesized star block copolymers during the current thesis. Chain extension of the star polymer was observed forming a diblock arm structure (Figure 9). However, a low molecular weight distribution was detected as well which is not desired. This low molecular weight distribution was not observed during the synthesis of star polymers containing only one MA or DEGA block. An experiment was performed comparing MA and DEGA chain extensions to investigate whether this is a process due to DEGA or not. As can be seen in Figure 9, the broad low molecular weight peak is however present in both conditions (pMA-*b*-pDEGA and pMA-*b*-pMA). Therefore a first suggestion would be the occurrence of an autopolymerization process of the present monomers independent of the desired controlled radical polymerization process synthesizing the desired diblock arm structures. Given the fact that this autopolymerization process occurs for both MA as DEGA monomers suggests that it is inherent to the 21-arm star polymer containing the first MA block.

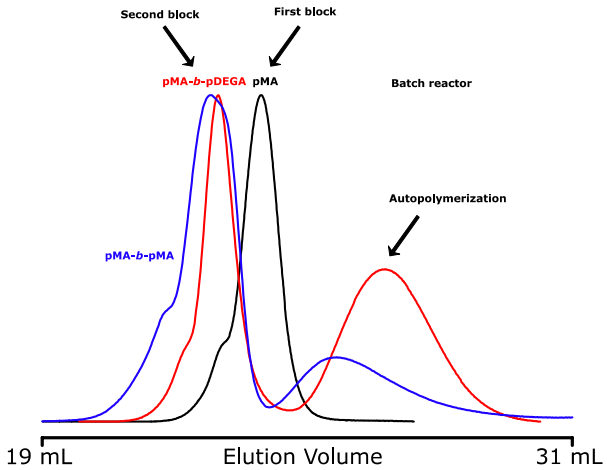

Figure 9: GPC traces of the chain extension for 21-arm star polymers with MA (blue) and DEGA (red) for polymerizations performed in batch. Reactions were performed for 90 minutes and arm lengths were targeted for 60 000 g·mol^{-1}. The [CH-Br]:[$Cu^{II}Br_2$]:[Me_6TREN]:[MA]/[DEGA] equivalents used were 1:0.01:0.075:319/697 with a monomer to solvent (DMSO) ratio of 1:15.

All these findings indicate that for chain extensions there is a certain mismatch in the reaction mixture. This could be caused by an incorrect estimation of the

molecular weight of the first star block copolymer by GPC. This incorrect estimation is due to the large discrepancy between measured and expected molecular weight for 21-arm star polymers (SI 1). However, for the experiments performed by Wenn et al on multiblock synthesis of 4- and 8-arm stars this behavior was not observed which states even more that the issues are originating from the 21-arm star polymer structure.[20]

A major consequence from these results is that the molecular weight of the total star cannot be correctly estimated by the used characterization methods (GPC and ^{1}H-NMR). It is uncertain how many monomers were incorporated in the diblock star polymer and how much was used for autopolymerization. Measurement of the molecular weight of the star polymer diblock structure via ^{1}H-NMR by conversion is therefore an overestimation. Furthermore, GPC will also incorporate the low molecular weight distribution in the estimation of the molecular weight of the star which will lead to high dispersity values. This will be explained in more detail in the next part demonstrating the synthesized thermo-responsive polymers.

Two strategies should envisioned for future experiments. First, methods for the removal of the undesired low molecular weight distribution should be explored. This can be performed by dialysis or by recycling GPC. The latter separates the present polymers in the crude polymer mixtures based on hydrodynamic volume. Therefore the star polymer which has a high molecular weight can be easily isolated from the total mixture. Secondly, methods towards correct estimation of the molecular weight of the star polymer containing the first MA block should be explored before chain extension is performed. This can be achieved as stated before by static laser scanning. Unfortunately this was not possible during this thesis since the necessary equipment for this type of measurement was not part of the available in house analysis equipment.

Further investigations in this behavior will be necessary to state that diblock synthesis was efficiently achieved without the presence of an additional autopolymerization event. However since the desired diblock structure was observed in GPC as a rather narrow distribution (indicating uniform star polymers) it is indicated that diblock synthesis of 21-arm star polymers will be very well possible.

3.2.2 Analysis of thermo-responsive properties

A range of different thermo-responsive star polymers was synthesized during this thesis. An overview is given in Table 2. Different lengths of MA and DEGA were targeted in order to investigate possible differences in LCST depending on the arm length. The additional low molecular weight distribution seen in Figure 9 was present in all synthesized diblock star polymer samples except for P1 (star polymer only composed of DEGA). As stated before the molecular weight analysis of these diblock star polymers should be regarded with a certain prudency. This is due to the presence of a low molecular weight distribution emerging during diblock

synthesis. This distribution was also included in the measurements and calculations to obtain the molecular weight and dispersity of the total diblock star polymer structures. Expected values that would be obtained by GPC after isolation of the desired star polymer would be performed are also given. These were obtained by neglecting the low molecular weight distribution and should therefore not be considered as conclusive results. Nevertheless similar values of the diblock star polymer structure would be expected when purification will be performed in future.

Table 2: Overview of the thermo-responsive star polymers synthesized in batch. The [CH-Br]:[$Cu^{II}Br_2$]:[Me_6TREN] equivalents used for all reactions were 1:0.01:0.075 except for the DEGA blocks of P5 and P6 using 1:0.02:0.12. The [CH Br]:[MA]/[DEGA] equivalents were calculated based on the targeted block lengths per arm with a monomer to solvent (DMSO) ratio of 1:15. Molecular weight (M_n) values were measured by GPC ($M_{n,\ corrected}$) and via monomer conversion obtained from ^{1}H-NMR ($M_{n,\ theoretical}$) taking the low molecular weight distribution into account if it is present (only absent for P1). The expected molecular weight values that would be obtained by GPC after isolation would be performed are also given.†

Polymer		MA block per arm	DEGA block per arm	Total star
P1	$M_{n,\ target}$ (g·mol^{-1})	-	20 000	
	Conversion (%)	-	45	
	$M_{n,\ theoretical}$[a] (g·mol^{-1})	-	9 000	193 300
	$M_{n,\ corrected}$[b] (g·mol^{-1})	-	10 300	219 900
P2	$M_{n,\ target}$ (g·mol^{-1})	5 000	60 000	
	Conversion (%)	58	70*	
	$M_{n,\ theoretical}$[a] (g·mol^{-1})	2 900	42 000*	947 200*
	$M_{n,\ corrected}$[b] (g·mol^{-1})	3 800	-*	197 500*
			22 200†	550 100†
P3	$M_{n,\ target}$ (g·mol^{-1})	10 000	20 000	
	Conversion (%)	75	68*	
	$M_{n,\ theoretical}$[a] (g·mol^{-1})	7 500	13 600*	447 400*
	$M_{n,\ corrected}$[b] (g·mol^{-1})	9 600	-*	61 600*
			18 300†	590 600†
P4	$M_{n,\ target}$ (g·mol^{-1})	10 000	10 000	
	Conversion (%)	75	66*	
	$M_{n,\ theoretical}$[a] (g·mol^{-1})	7 500	6 600*	300 400*
	$M_{n,\ corrected}$[b] (g·mol^{-1})	9 600	-*	36 200*
			9 600†	408 100†
P5	$M_{n,\ target}$ (g·mol^{-1})	10 000	30 000	
	Conversion (%)	75	61*	
	$M_{n,\ theoretical}$[a] (g·mol^{-1})	7 500	18 300*	546 100*
	$M_{n,\ corrected}$[b] (g·mol^{-1})	9 600	-*	114 300*
			30 900†	854 400†
P6	$M_{n,\ target}$ (g·mol^{-1})	12 000	60 000	
	Conversion (%)	69	63*	
	$M_{n,\ theoretical}$[a] (g·mol^{-1})	8 300	37 800*	971 900*
	$M_{n,\ corrected}$[b] (g·mol^{-1})	8 900	-*	90 400*
			15 000†	507 200†

[a]M_n calculated via conversion obtained by ^{1}H-NMR. [b]M_n measured by GPC and multiplied with a correction factor (2.73) taken from literature[48]. For sequence extension a low molecular weight distribution was observed in GPC aside from the desired star polymers. *M_n values calculated taking the low molecular weight distribution into account. †M_n values that should be expected after removal of the low molecular weight distribution.

Calculation of the theoretical molecular weight of the star polymers is based on conversion determined via ^{1}H-NMR. Values for samples containing the low molecular weight distribution (P2, P3, P4, P5, P6) are an overestimation since more monomer is consumed then is incorporated in the star polymer. This originates from the fact that the measured monomer conversion is the sum of the conversion of the undesired autopolymerization and of the conversion from the diblock star polymer. Contrarily due to the same effect, much lower molecular weight values were measured by GPC. Aside from the known concerns regarding the measurement of the molecular weight of star polymers by GPC (as mentioned earlier), this is explained by the fact that the low molecular weight distribution will decrease the number average weight of the polymers present. In other words, the presence of a low molecular weight distribution together with the high molecular weight diblock star polymers leads to a decreased measured molecular weight since the measurement method takes both polymer distributions into account.

Another consequence of the presence of the low molecular weight distribution is that rather high dispersity values are obtained. P1 is an exception since it is only composed out of DEGA and does not possess a diblock structure or an additional low molecular weight distribution ($Đ$ = 1.16). For this reason the dispersity values were not reported in Table 2. However after purification which removes the low molecular weight distribution, only the narrow star polymer distribution should remain. When remeasuring this sample low dispersity values should be acquired indicating that uniform star polymer diblock structures are obtained. Also the molecular weights that would be obtained from GPC hereafter are expected to approximate the values that were obtained by neglecting the presence of the low molecular weight distribution (Table 2, values in grey[†]). Nevertheless, purification strategies should be envisaged to obtain pure and uniform star polymer structures. In this regard the diblock star polymers can be isolated by dialysis or recycling GPC as mentioned before.

In Figure 10 the LCST measurement of the polymers shown in Table 2 is given. The thermoresponsive behavior was characterized by measuring light transmission at 500 nm at various temperatures (Figure 10, a). Below the characteristic LCST, the polymer solutions were transparent indicating dissolution of the star polymer which leads to a high transmittance value. Upon heating, the enthalpy (interaction of water molecules with the polymer) no longer compensates for the loss of entropy of the water molecules surrounding the polymer. This leads to a Gibbs free energy of zero at the LCST. This is visually observed by clouding or increase in turbidity of the polymer solution. Which possibly is due to agglomeration of multiple star and/or linear polymers (Figure 10, b) which expresses itself in a low transmittance value.

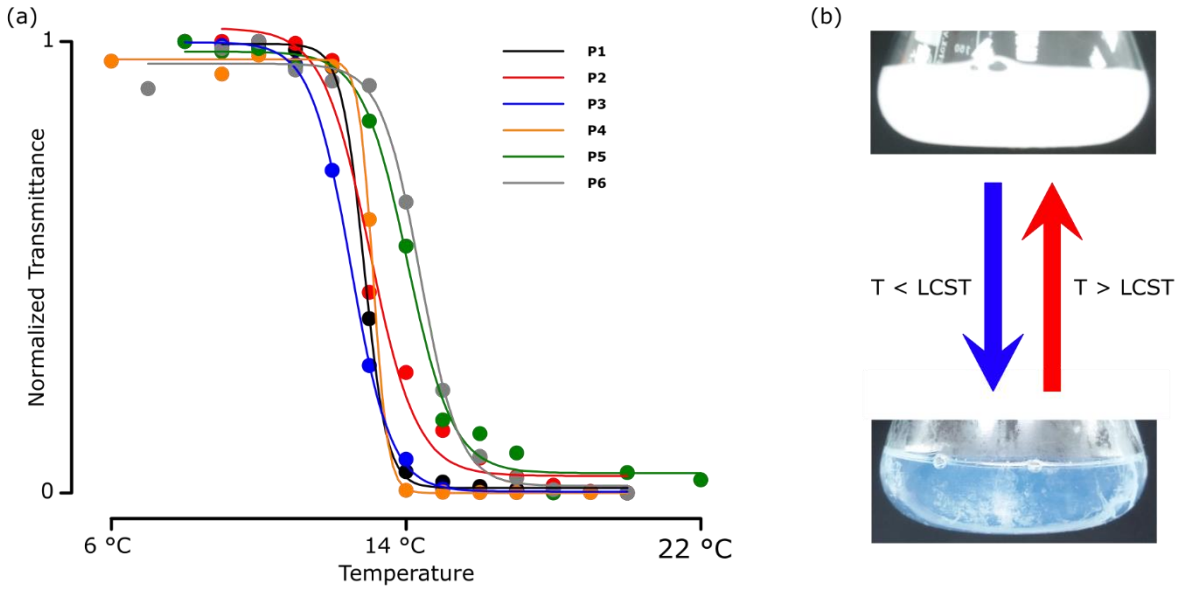

Figure 10: Detection of the LCST for the polymers from Table 2 by measurement of the transmission of light at 500 nm at various temperatures (a). The response can be observed visually as an increase in turbidity above the LCST (b). Polymer solutions were 0.5 wt% in H_2O and transmission values were normalized.

Concerning star polymer P1 (only composed of DEGA, Table 2) a rapid temperature response is observed around 14°C. This value is consistent when compared with studies on linear analogues.[28] Herein, the DEGA monomer is reported to lead to an LCST of around 13 °C. However, tuning of this temperature is shown to be possible by polymerizing a mixture of two monomers of which the different homopolymers would possess a distinct LCST when polymerized separately. Hydroxyethylacrylate (HEA) for example has an LCST above 100 °C and is therefore more hydrophilic then DEGA. Copolymerizing this monomer with DEGA in a specific ratio is proven to lead to higher LCST temperatures (up to 38.5 °C) with increasing amount of HEA.[28] A comparable strategy should be envisioned in future experiments to increase the LCST since the current conditions are of course not favorable for biological applications.

LCST measurements of the remaining star polymer samples gave similar results (Figure 10, a). However as mentioned before, these polymer samples contain an additional low molecular weight distribution which indicates the presence of a certain fraction of linear pDEGA polymer. It is at this moment not yet clear whether this fraction disturbs the LCST or not. Nevertheless, given the fact that star polymer P1 (only composed out of DEGA and absence of the low molecular weight distribution) possesses a clear temperature response demonstrates that thermo-responsive star polymer structures can be synthesized. At this stage no conclusive statement on the LCST and the thermo-responsive property of the synthesized diblock star polymers (containing the additional low molecular distribution) can be made. What can be stated is that regardless of the presence of the low molecular weight distribution, these samples were dissolved in water below 14 °C and that these suspensions possessed a certain temperature response. However, measurement of the characteristic LCST specifically for the star polymers alone was not yet possible. Therefore, in future the synthesis procedure for diblock star

polymers should be optimized to prevent auto polymerization. Alternatively the prepared diblock star polymer samples can be purified to isolate the desired star polymers. This purification could be performed as mentioned before by recycling GPC or dialysis.

It should be noted as well that the current technique to measure the LCST is adequate to show a trend of the thermo-responsive behavior. However in order to produce conclusive results these samples should be measured on a different instrument capable of measuring and controlling the temperature during transmittance measurements. In the current thesis this was performed manually by measuring an absorbance spectrum at each temperature incline of the aqueous polymer suspension. Alternatively, a different approach can also be targeted in future experiments via differential scanning calorimetry or diffusion ^{1}H-NMR since the LCST is accompanied by an endothermic peak and a decreased diffusion constant.

Synthesis of 21-arm star polymers with a diblock arm structure is a topic of further optimization concerning characterization and synthesis procedures. Therefore when this is performed during future investigations, the thermo-responsive property of these star polymer structures can be correctly assessed. The LCST of star polymers with arms composed solely out of DEGA was however evaluated showing that these star polymers can be given a thermo-responsive character.

3.3 End group modification

When considering biomedical applications, the star polymer should be functionalized. Figure 11 shows an overview of the explored and envisioned strategies. For future applications targeting modalities (small peptide sequences) should be attached to direct the star polymer towards a desired location. Direct peptide synthesis on the surface of the star polymer is in this regard an aim for future investigations. To enable such strategies, a primary amine end group is a requirement in the first place. Therefore the primary amine was one desired end group modification. Furthermore attachment of fluorescent molecules could be envisioned as well to allow (bio)imaging as another potential application. This can be achieved via click chemistry. Hence the presence of an azide end group was another goal since it will allow for copper(I) catalyzed alkyne-azide cycloaddition (Cu^{I}AAC) click chemistry.

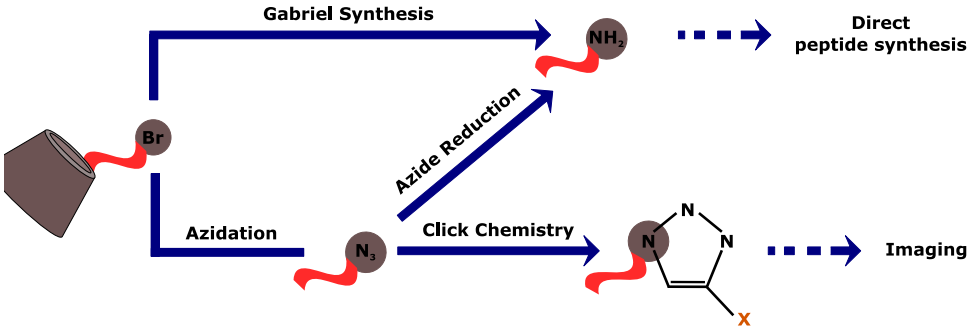

Figure 11: General overview of the intended end group modifications of star polymers synthesized by photoCMP and the chemical pathways to be followed. Envisioned future applications are also given.

As a consequence of the used controlled radical polymerization method, the star polymers show a high end group fidelity. In the present case this means that after polymerizations the star polymers possess and maintain a bromine atom as end group (Figure 11). These bromine atoms can be exchanged for other useful chemical moieties. The modifications were first performed on a linear polymer (pMA synthesized via photoflow in the homemade 2 mL PFA flow reactor, M_n = 1 600 g·mol^{-1}, $Đ$ = 1.12) since this was easier to confirm by in house characterization techniques such as ESI-MS and ^{1}H-NMR. Therefore, the assumption was made at this stage that when the explored transformation strategies are achieved on linear polymers they should be translated easily towards star polymers when ideal reaction conditions are established.

3.3.1 Azidation and consecutive Cu^{I}AAC

First, the bromine group was modified into an azide via a nucleophilic substitution by stirring with NaN_3 for 5 hours at room temperature. The followed reaction pathway is shown in Scheme 1 (a). Effective modification was observed by ESI-MS (SI 3). This end group modification was envisioned among others since it can be used for the attachment of fluorescent probes or targeting functionalities via click chemistry. A consecutive Cu^{I}AAC click reaction (overnight at room temperature) of the linear polymer with *N*-Boc-propargylamine was performed to verify this possibility (Boc = *tert*-butyloxycarbonyl, an amine protecting group). The used reaction strategy is shown in Scheme 1.

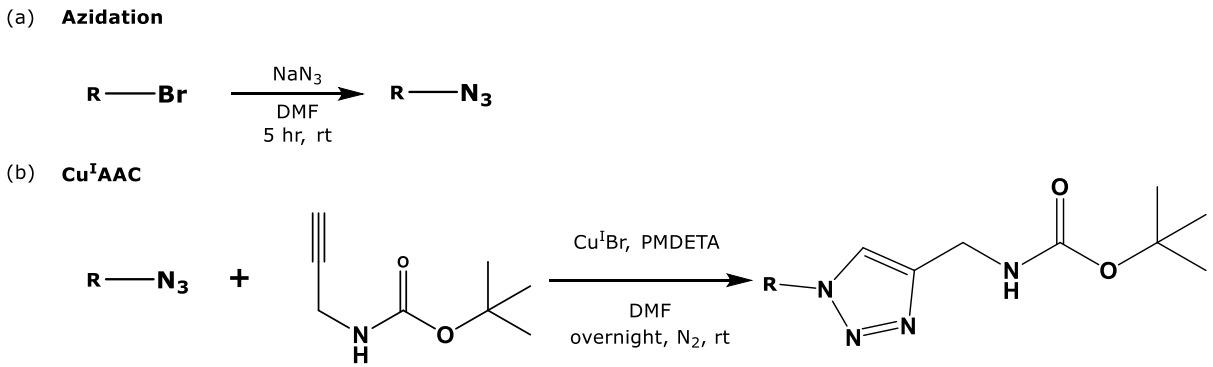

Scheme 1: Summary of the procedures that were followed for azidation (a) and the consecutive Cu^{I}AAC reaction to attach *N*-Boc propargylamine. The polymer chains containing the end groups are represented by "R".

The attached *N*-Boc propargylamine can later be additionally transferred into propargyl amine. Figure 12 shows the ESI-MS result of this click reaction after transforming the bromine end group into an azide. In the full mass/charge (m/z) spectrum two main distributions are observed (Figure 12, a). These are attributed to single charged (largest distribution) and double charged (smaller distribution) species after comparing the expected and measured m/z peaks (Figure 12, b, c and d). Furthermore the distance between two m/z peaks is exactly the mass of one monomer (MA, 86.04 g·mol^{-1} for single and 43.52 g·mol^{-1} for double charged species, Figure 12, b) The attachment of *N*-Boc-propargylamine was also indirectly observed by GPC as manifested by an expected shift of the distribution to higher molecular weights (from 1 600 g·mol^{-1} to 1 900 g·mol^{-1}, SI 4).

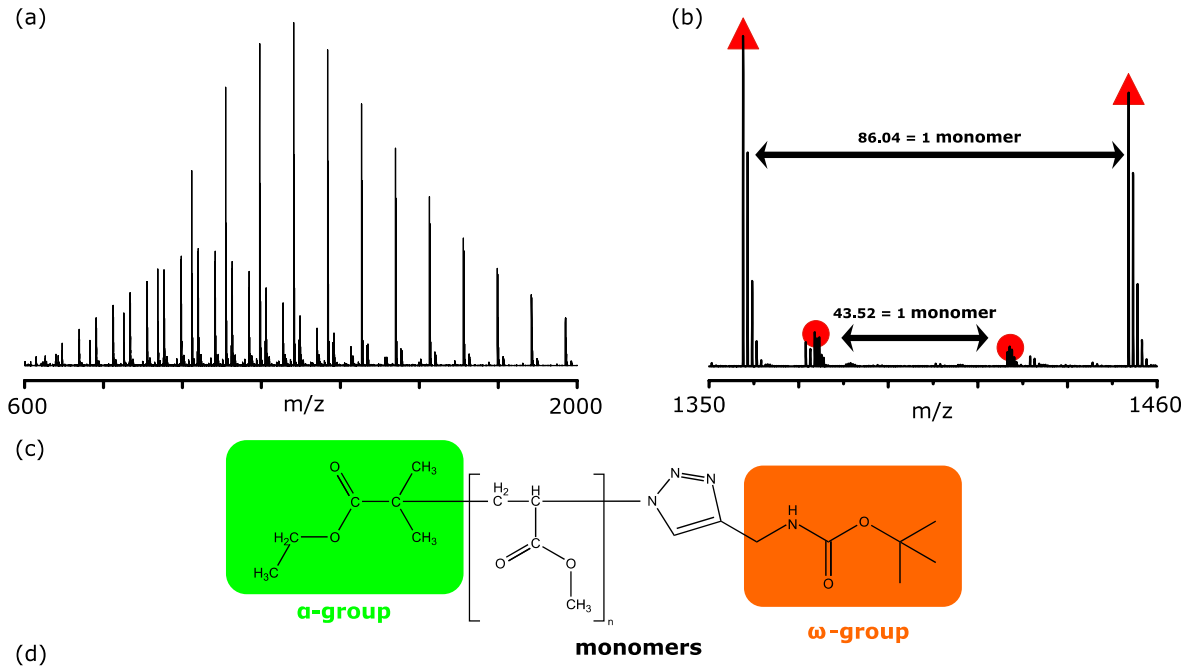

α-group	ω-group	Number of monomers	Ion	$m/z_{, th}$	$m/z_{, exp}$
▲ EBiB	NH-Boc	11	Na^+	1367.61	1367.61
▲ EBiB	NH-Boc	12	Na^+	1453.65	1453.64
● EBiB	NH-Boc	27	$2Na^+$	1383.60	1383.59
● EBiB	NH-Boc	28	$2Na^+$	1426.61	1427.11

Figure 12: ESI-MS analysis of the Cu^{I}AAC of linear polymers with *N*-Boc-propargylamine. The full ESI-MS spectrum (a) and spectrum of single monomer repeating units (b) are given. Triangles and circles respectively represent single and double charged species. The different theoretical and experimental mass/charge (m/z) values of the synthesized structure (c) are given in (d). Cu^{I}AAC was performed overnight at room temperature under nitrogen atmosphere using [CH-N_3]:[Cu^{I}Br]:[PMDETA]:[*N*-Boc propargylamine] equivalents of 1:2:4:2.

The above established azide end group transformations and click reactions were performed following batch procedures, however continuous flow methods were also shown to be possible by previous findings in our group.[40]

Translation of these findings (azide) on linear polymers towards star polymers was explored as well. However, presence of the azide as an end group as well as the consecutive click reaction (overnight at room temperature) of the star polymer could not be directly observed at this stage. The limiting factor lies currently in determining the presence of an azide as end group of the star polymers. Straightforward verification of this condition via ESI-MS is not possible since the star polymer structure has a molecular weight above the measurable m/z window (m/z up to 2 000). Nevertheless, these are established reaction procedures and successful transformation of the bromine to an azide end group on linear polymers was achieved. Therefore, this end group modification will be possible as well for star polymers. This is a highly interesting end group since it allows for the attachment of a plethora of additional functionalities on the star polymers as shown by the attachment of *N*-Boc propargylamine to linear polymers.

3.3.2 Exploration of amination strategies

A primary amine as end group is desired when aiming for future applications in which the star polymers are used as thermo-responsive supports for direct peptide synthesis. By using this technique specific targeting sequences can be grown on the surface of the star polymer. Several approaches were investigated during this thesis to implement such an end group. Scheme 2 briefly summarizes the different reaction pathways that were tested during this thesis.

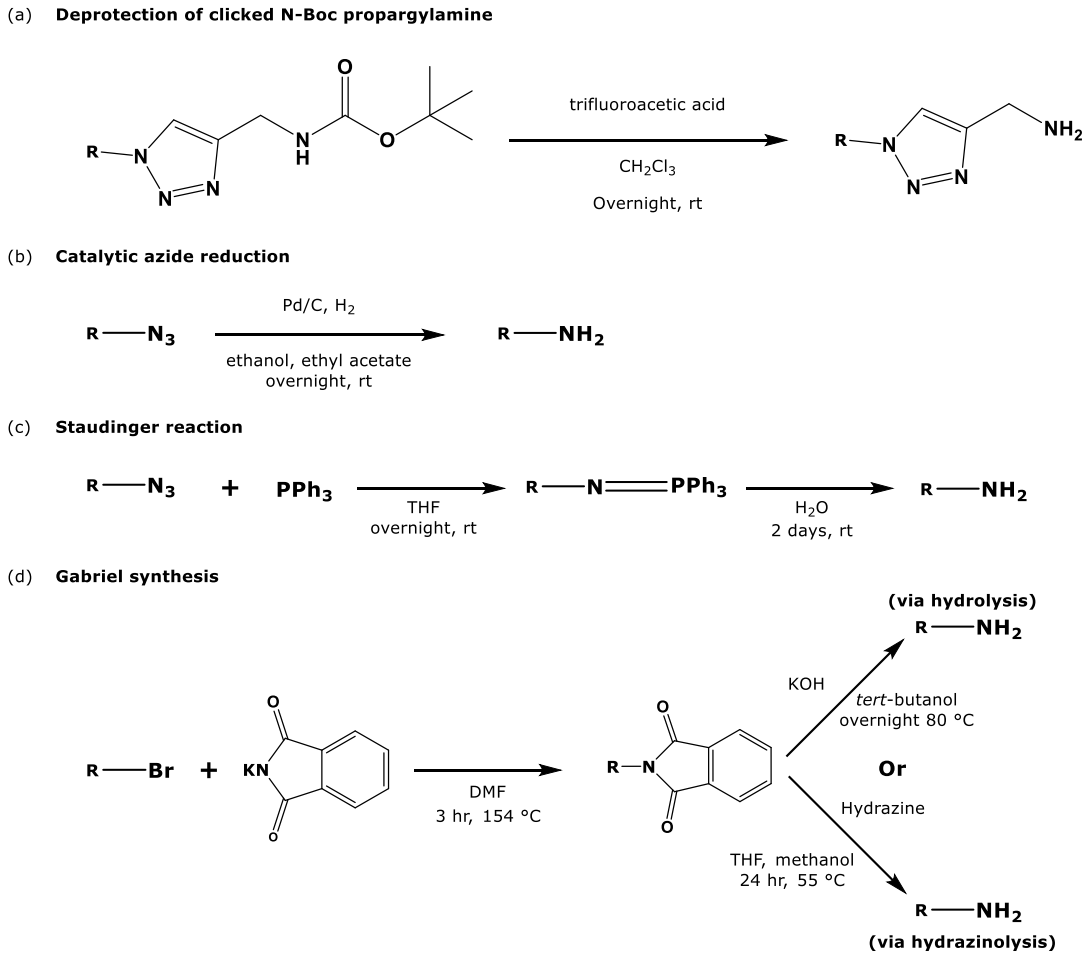

Scheme 2: Brief summary of literature known and tested strategies during this thesis to introduce a primary amine as endgroup.

The different pathways were also in this part first explored on linear polymers since analysis is more practical. Nevertheless, translation of these strategies towards star polymers is expected to be straightforward when the ideal reaction conditions are established.

As shown in Figure 12, *N*-Boc-propargylamine was attached to azide end group modified linear polymers. The amine protecting Boc-group can be removed by following a mild deprotection procedure (overnight stirring with trifluoroacetic acid at room temperature, Scheme 2, a).[55] The ESI-MS analysis of the polymers after deprotection is given in SI 5 which mainly shows the presence of primary amine end group modified linear polymers. Presence of other structures such as still protected amine groups was also observed. Further optimization of the

deprotection procedure is therefore necessary to ensure complete removal of the protection groups. Different combinations of reaction times and amounts of trifluoroacetic acid can be tested. Nevertheless, introduction of an amine end group via this route was shown to be possible.

Despite the successful introduction of an amine end group via Cu^{I}AAC of *N*-Boc-propargylamine other direct and more elegant pathways to generate amine end groups were investigated. In this regard several methods are known from literature starting from an azide or a bromine end group. Catalytic reduction of the azide end group using palladium and hydrogen gas is a rather harsh approach (Scheme 2, b).[56] When exploring this route not only the azide end group was reduced but also the ester functionalities in the pMA polymer were affected. The resulting ESI-MS spectra therefore showed a high unassignable peak density. Milder approaches were therefore explored such as the Staudinger reaction which employs triphenylphosphine (PPh_3) to selectively reduce the azide functionalities (Scheme 2, c).[57] Nevertheless, the desired amine end group modified polymers were never obtained as indicated by the absence of the desired polymer distribution in the measured ESI-MS spectra after multiple trials.

A completely different approach to get a primary amine as functional end group is the Gabriel synthesis of amines directly from bromine atoms using potassium phtalimide salt (Scheme 2, d).[42] This is a two-step procedure by which the first step exchanges the bromine atom for a phtalimide group (3 hours at 154 °C). In Figure 13 (a) the NMR spectrum is given before (black line) and after (red line). Herein, an expected shift of the proton near the bromine/phtalimide to higher ppm is observed due to a change in the surrounding chemical environment of this proton. In the second step of the Gabriel synthesis pathway, the phtalimide end group can be cleaved off by hydrolysis using KOH or by hydrazinolysis. Hydrolysis by KOH led once more to degraded polymer and for this reason the attention was focused towards the hydrazinolysis route. The ESI-MS spectrum of the end group modified polymers synthesized by removal of the phtalimide group using hydrazine (24 hours at 55 °C) is shown in Figure 13 (b).

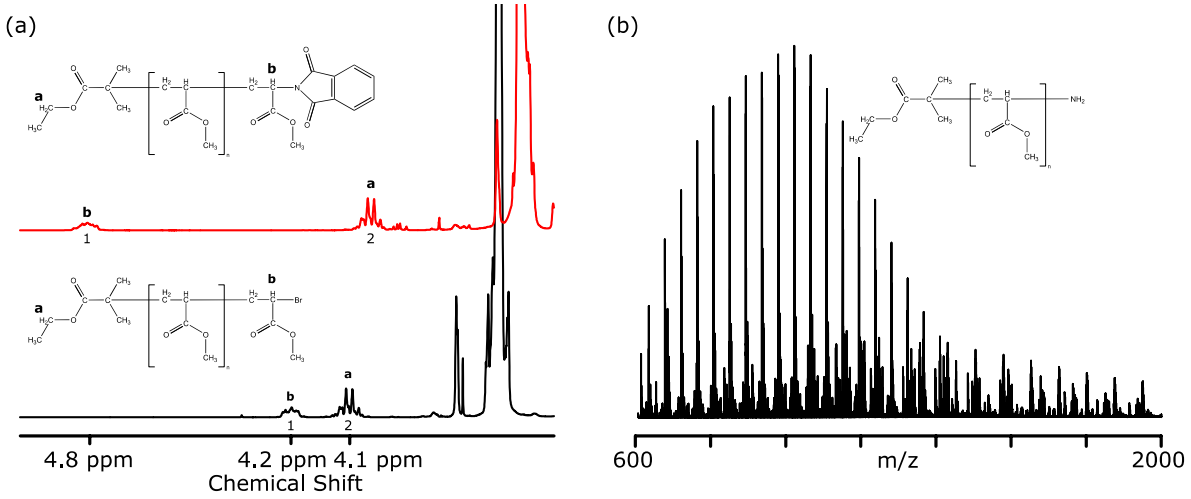

Figure 13: Results of gabriel synthesis to introduce primary amine end groups on linear polymers. ^{1}H-NMR spectrum (measured in $CDCl_3$) of the first step in the Gabriel Synthesis on a linear polymer before (bottom) and after (top) a phtalimide end group was introduced (a). In the second step the phtalimide group was cleaved of by hydrazinolysis yielding amine end group modified polymers as observed by the main distribution observed in ESI-MS (b). The first step was performed with [CH-Br]:[potassium phtalamide] equivalents of 1:1.1 by refluxing for 3 hours at 154 °C. The second step was performed with [CH-phtalamide]:[hydrazine monohydrate] equivalents of 1:5 by refluxing for 24 hours at 55 °C.

After hydrazinolysis the measured ESI-MS spectrum contained a main distribution which was established to originate from double charged amine end group modified polymers (Figure 13, b). In SI 6 the ESI-MS spectrum focusing on a single monomer repeating unit is also given. From these two spectra it can be seen that despite the major presence of amine end group modified polymers a minor distribution can be observed as well which indicated the presence of several impurities and incompletely end group modified polymers. Even with the present difficulties this route has presented itself as the most promising in the generation of a primary amine end group. Optimization of this reaction will therefore be topic of future investigations in which different reaction times, equivalents of hydrazine monohydrate, and temperatures should be examined to minimize side product formation.

In this part strategies were explored to modify the chemical end groups of the star polymer towards other interesting functionalities. These strategies were explored on linear polymers since end group analysis is more straightforward on linear polymers compared with star polymers. Azide end group modified linear polymers were realized together with a successive Cu^{i}AAC click reaction. After testing several literature procedures (e.g. catalytic reduction and Staudinger reduction) the generation of an amine end group proved to be challenging. Most promising results were obtained by Gabriel synthesis which yielded the most promising results. Furthermore, since this route starts directly from the bromine end group a one-pot strategy could be envisioned in the future when the explored strategies are effectively translated to star polymers. In this regard the azide as well as the phtalimide end groups are formed simultaneously on the surface of the star polymer. After hydrazinolysis the present phtalimide end groups, the star polymer shall possess two different surface functionalities (e.g. azide and primary amine) combined into one molecule which can be used for two different applications

(e.g. direct peptide synthesis and attachment of fluorescent functionalities, Figure 11). This will demonstrate the versatile character of the star polymers.

3.4 Explorative study of the bio(medical) potential

In the end the aimed applications should be addressed to demonstrate the feasibility of using star polymers in bio(medical) research and/or bio-applications. Potential applications of the star system are for instance, candidate drug carrier (by entrapping a drug), targeted delivery (by engineering the arms with specific sequences) or (bio)imaging (by attaching a fluorescent marker). Therefore, this potential was assessed in an explorative study to estimate the future potential. It should be noted that the following experiments were performed using the thermo-responsive diblock star polymers that were created during this thesis. As mentioned before, these star polymers were shown to contain an additional low molecular weight distribution which will be absent after purification or optimization of the synthesis procedure. Nevertheless, the desired star polymer structures were present with a higher abundancy which allows for a proof-of-concept study to gain insight in the biomedical potential of these star polymers.

3.4.1 Loading of hydrophobic dye and size measurement

Drug delivery has been mentioned as one of the applications for star polymers in this thesis. However, before enabling delivery and drug release the loading of hydrophobic drugs onto the synthesized star polymers should be investigated. Several groups before presented the succesful loading of hydrophobic molecules into amphiphilic star polymers.[25-26,58-59] The loading potential of star polymers synthesized during this thesis composed of a hydrophobic inner structure and hydrophilic mantle was tested with the fluorescent rhodamine B dodecyl ester dye. The used dye is hydrophobic and presents itself as ideal testing compound for the loading of hydrophobic molecules. An experiment was performed by using a 0.1 wt% suspension of P3 (Table 2) loaded with 10 ppm fluorescent rhodamine B dodecyl ester at 0 °C for 30 minutes. Figure 14 reveals the results on the dye loading experiment as well as DLS measurements of the selected star polymer (P3,Table 2).

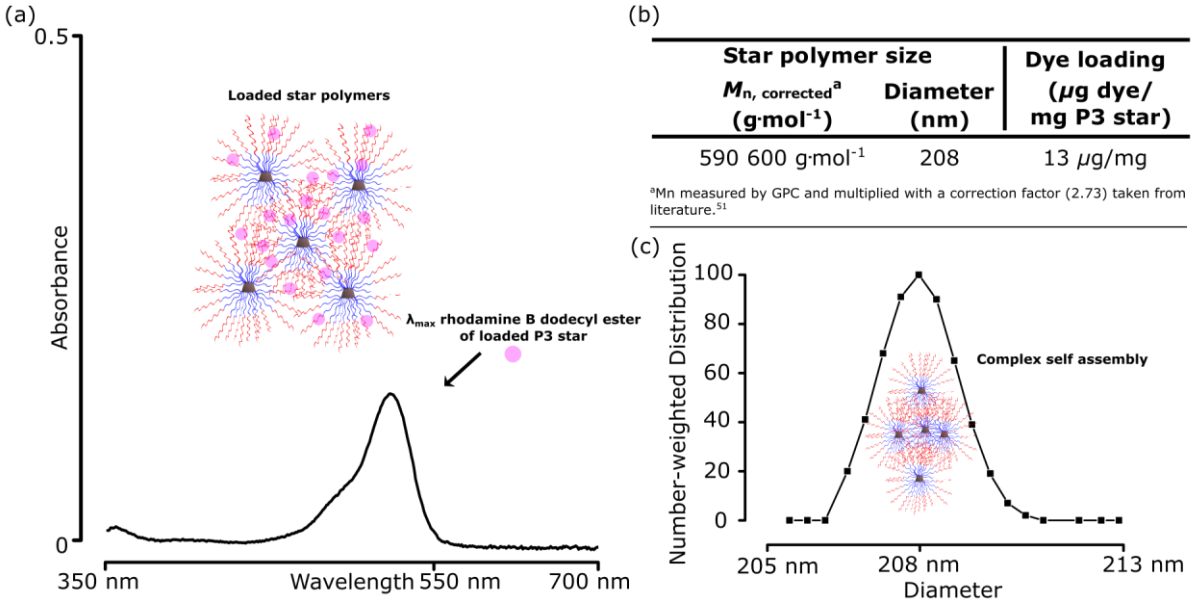

Figure 14: Absorbance spectrum of the star polymers after loading with rhodamine B dodecyl ester (a). Properties of the star polymer (P3, M_n = 590 600 g·mol^{-1}, Đ = 1.15) as well as the amount of dye loaded are given in (b). Dye loading was calculated against a standard calibration curve (SI 7) and the particle size distribution of complex self-assemblies of star polymers was measured by DLS (c) with a concentration of 0.1 wt% P3 in H_2O.

After loading the dye onto the star, the absorption spectrum of the loaded fraction (star-drug entrapment) showed an absorbance peak (λ_{max} = 544nm) characteristic for rhodamine B dodecyl ester (Figure 14, a). The dye was further quantified by means of fluorescence measurement (excitation at 544 nm) and the fluorescence value was measured against a standard calibration curve (SI 7) to determine the amount of dye which was loaded in the P3 star polymer. This quantification suggested that 13 *μ*g of the rhodamine dye was loaded onto 1mg of the P3 star polymer (Figure 14, b). However, this experiment should be verified by further experiments when star polymer diblock synthesis has been optimized (removal of the earlier stated low molecular weight distribution). Additional investigations should be conducted on the release behavior of the loaded star polymers. Also loading and release experiments with different blind tests have to be done. Herein it should be tested whether star polymers with arms composed solely of MA or DEGA are also able to load a certain amount of hydrophobic cargo. This will give further indications whether the presence of a diblock arm structure is beneficial or not for the entrapment and controlled release of the cargo. Furthermore, the β-CD core molecule of the synthesized star polymers is known to possess an additional entrapment possibility on its own. Individual cyclodextrin molecules can provide a favorable environment for water insoluble drugs in their hydrophobic cavity due to its specific structure. This allows drugs to be completely or partially included in the cyclodextrin molecule.[60] Whether, the drugs are included in the hydrophobic cavity of the β-CD core or are trapped in the inner part of the star polymer should be further investigated as well for instance by two-dimensional ^{1}H-NMR techniques.

The P3 star polymer *(*Table 2) was also characterized by DLS with a diameter (D_{50}: diameter at 50% of a cumulative distribution) of 208 nm. This suggests that a certain complex self-assembly behavior is present which leads to the formation of

micelles. This might increase the amount of cargo that can be loaded. Complex self-assembly behavior has been observed before in literature on β-CD core star polymers composed of pNIPAM.[53] For future investigations when star polymer diblock synthesis has been optimized, this complex self-assembly behavior should be studied in more detail. In this regard the CMC will be also investigated, which is the specific concentration at which the formation of micellar structures is realized. This CMC can be established via surface tension measurements or via DLS by measuring the count rate and hydrodynamic volume at different concentrations of the star polymer suspension in aqueous environment.

Measurement by DLS over time was also performed and the results are shown in SI 8. In this measurement the agglomeration behavior above the LCST can be observed by the appearance of a bimodal distribution. This distribution starts to emerge after longer measurement times in which the aqueous polymer sample approaches room temperature surpassing the LCST of the polymer (around 14 °C).

As a summary, the outcome of the preliminary rhodamine dye loading experiment showed positive first indications on the loading of the star polymers with a hydrophobic substance. Further experiments investigating the release behavior as well as comparing the findings with different blind tests should be performed when optimal star polymer synthesis is achieved. For future loading experiments, an additional method for instance spin column based size exclusion chromatography or high speed centrifugation should be employed in purification steps to ensure complete removal of unloaded components from the star containing dye fraction. When these loading experiments are established with the rhodamine dye the translation of these findings to actual hydrophobic drugs will be performed. Herein doxorubicin (a known anti-cancer therapeutic) could be used which has beside a high cytotoxic activity also an inherent fluorescent capacity.[61] This fluorescence behavior is ideal for the quantification of the amount of loaded drugs inside the star polymer. Afterwards these experiments should be repeated in a biologically realistic environment such as physiologic buffer solution (e.g. phosphate buffered saline) or cell medium in order to observe the impact of such an environment on the drug loading and release behavior of the star polymers. In this regard protein corona studies are also an experimental aim. When this detailed knowledge has been obtained the goal of drug delivery will be another step closer.

3.4.2 Attachment of fluorescent polymers for future (bio)imaging

As a final part, the potential of star polymers for (bio)imaging purposes was briefly explored. This was done by investigating the attachment of a fluorescent alkyne modified poly[2-methoxy-5-(3’,7’-dimethyloctyloxy)-1,4-phenylene-vinylene] (MDMO-PPV) block to azide end group modified thermo-responsive star polymers (P6, Table 2) via Cu^{I}AAC (8 days stirring at room temperature). This experiment was performed as a qualitative investigation to observe whether a fluorescent marker can be attached to the star polymer. The MDMO-PPV polymers gain their fluorescent capacity due to their conjugated structure (alternating double bonds). Originally these materials have been developed for possible opto-electronic

applications (e.g. photodiodes). However, their potential to perform in biomedical applications for (bio)imaging is currently being explored by the Junkers group. These materials have recently gained interest for imaging purposes particularly due to absence of significant photobleaching of the fluorescent structure. Concerning these applications, PPV containing micelles[62] and nanoparticles[63] have been used by Zaquen et al and Peters et al. The formation of star polymers containing fluorescent PPV materials would add another polymer architecture to the existing toolbox for (bio)imaging applications using PPV materials.

Figure 15 shows the GPC traces of "clicked" and "unclicked" star and MDMO-PPV polymers (blue line), together with the isolated "clicked" star polymers by utilizing the thermo-responsive property of the star polymer (red line). The GPC trace of the unclicked star MDMO-PPV polymers is also given (black line).

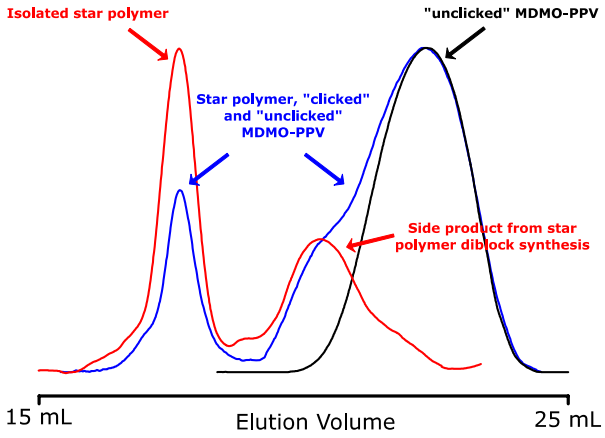

Figure 15: GPC traces of star polymers after $Cu^{I}AAC$ with alkyne modified MDMO PPV blocks together with the isolation of the star polymers from the crude polymer mixture. GPC trace of MDMO-PPV blocks is given (black line) as well as the crude mixture after reaction (blue line) containing "clicked" and "unclicked" star polymers as well as unreacted MDMO-PPV polymers. The low molecular weight distribution due to auto polymerization during star polymer synthesis was also observed. Star polymer isolation was attempted by exploiting the thermo-responsive property of the star polymers by filtration of a cooled water solution (4°C) of the crude polymer mixture (red line).

The star polymer containing the MDMO-PPV functionalities after $Cu^{I}AAC$ had to be isolated from the crude polymer mixture since assessing the fluorescent character of this mixture (Figure 15, blue line) would be incorrect. This isolation was done in an aqueous environment utilizing the thermo-responsive property of the star polymers. The hypothesis is that only the star polymers ("clicked" and "unclicked") will be dissolved in an aqueous polymer mixture that was cooled below the LCST (4°C), while the unreacted hydrophobic MDMO-PPV polymers will not. Therefore these MDMO-PPV polymers will stay behind in the filter during filtration of this cooled aqueous mixture. This isolation of the star polymers functionalized with a certain amount of MDMO-PPV was examined by GPC (Figure 15, red line). The GPC result showed only the star polymer and the accompanying low molecular weight bump observed for the thermo-responsive star polymers (shown in Figure 9 and as discussed previously) after filtration. Nevertheless, at this stage the presence of a certain rest fraction of unreacted MDMO-PPV should not be excluded. Therefore in further investigations the isolation by exploiting the

thermo-responsive property of the star polymer should be compared with established techniques such as recycling GPC which can separate the crude polymer mixture based on the differing hydrodynamic volumes of the present polymer structures ("clicked" and "unclicked" star polymers and unreacted MDMO-PPV polymers).
The absorbance spectrum shown in Figure 16 was recorded of the isolated star polymers by exploiting the thermoresponsive property of the star polymers. The characteristic peaks of MDMO-PPV were observed after isolation which suggests that a certain fluorescent property was introduced in the star polymer. As stated earlier the complete removal of unreacted MDMO-PPV polymers (which also exhibit a fluorescent respons) should not be totally claimed. However, attachment of a certain amount of fluorescent polymers is still rather likely. Quantification of this process should be envisioned in the future which can be achieved calculating the amount of reacted MDMO-PPV materials against a standard calibration curve.

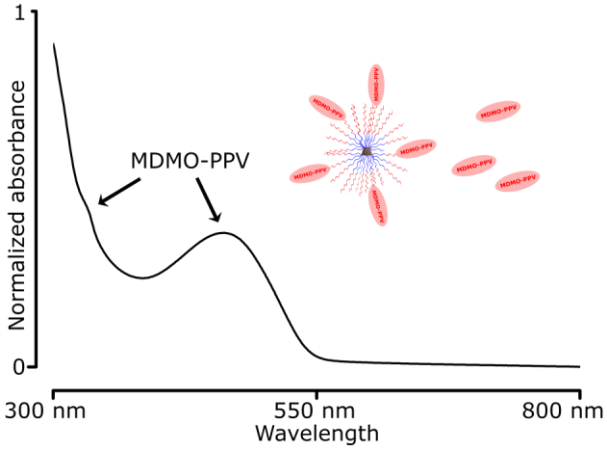

Figure 16: Absorbtion spectrum of the star polymers after $Cu^{I}AAC$ with alkyne modified MDMO-PPV blocks and attempted isolation of the star polymers from the crude polymer mixture by exploiting the thermoresponsive property of the synthesized star polymers, presence of unclicked MDMO-PPV polymers is not excluded.

The fluorescent signal of the MDMO-PPV attached star polymer after $Cu^{I}AAC$ was further observed by fluorescence measurements. These functionalized star polymers were excited at 485 nm and the emission of the fluorescent signal was observed at 590 nm. The preliminary result revealed fluorescence of the MDMO-PPV attached star polymer, while the unclicked star polymers possessed virtually no fluorescent character (SI 9). As stated before the possible presence of unreacted MDMO-PPV even after attempted isolation should not be ignored. Further efforts should be performed on the purification (e.g. by recycling GPC) of the crude polymer mixture after $Cu^{I}AAC$. Afterwards the generation of star polymers functionalized with fluorescent polymers can be completely confirmed when a fluorescent character is still observed. The amount of attached fluorescent MDMO-PPV polymers can then be quantified via a standard curve. Complete attachment fluorescent polymers to all functional end groups is in this context not the aim since the remaining unreacted functional groups could then be still used for further functionalization such as the attachment of other substances (e.g. targeting functionalities).

The current findings suggest that star polymers hold promise for the future functionalization with fluorescent modalities (i.e. fluorescent MDMO-PPV polymers). However, further conclusions are at this stage not yet possible. Nevertheless when the procedures are optimized the star polymer can be used for (bio)imaging purposes. This can be achieved by varying the reaction times and equivalents of the used reagents. Furthermore recycling GPC can be used to improve the isolation of the functionalized star polymers from the unreacted MDMO-PPV polymers. The results from this methodology (recycling GPC) should then be compared with the isolation method/procedure exploiting the thermo-responsive property. Furthermore, the latter procedure will offer/facilitate a more convenient approach for purification once optimized. Extensive research on PPV as nanoparticle and fluorescent micelles is currently carried out at the research groups of Junkers and Ethirajan.[62-63] In addition, when the current system (star polymers functionalized with MDMO-PPV) and the reaction contitions are fully optimized, this investigation will allow the star polymer to be further used in an extended field of biological applications, particularly (bio)imaging.

4 Conclusion and Outlook

The current work contributed to the fundamental first work on star shaped polymers, taking a first step towards an advanced material to be used in the field of nanomedicine. Star polymers are highly versatile materials combining multiple properties into one molecule. Existing work in our labs on these structures was further elaborated during this thesis. The performed research was constituted out of three pillars. First, the implementation of a temperature response was investigated. Secondly strategies towards modification of the end groups of these star polymers were explored. Finally, the potential biomedical applications were investigated briefly in the last part.

Star polymers with up to 21 arms were synthesized with photoCMP using batch and continuous flow procedures. The amount of copper species is brought down to ppm concentration which is highly favorable when aiming for biomedical applications. Furthermore, due to the benefits of (photo)CMP diblock arm structures could be realized using MA as inner hydrophobic layer and DEGA as outer thermo-responsive shell. However the presence of a certain low molecular weight distribution due to autopolymerization was also observed. Strategies to prevent this formation should be explored in further investigations. Otherwise removal of this peak can be envisioned by recycling GPC to isolate the formed star polymers containing diblock arm structures. A thermo-responsive behavior of these star polymers was nevertheles observed by clouding of an aqueous polymer solution occurring around 14 °C regardless of the presence of this additional polymer distribution. Additionally, the use of DEGA will also introduce an antifouling property in the star polymer. This will most likely minimize detrimental protein corona formation when examining star polymer behavior in biological environments in future experiments. Despite the fact that synthesis of star polymers has shown to be rather tedious, positive indications are given which stimulate further investigations to obtain pure and uniform star polymer structures.

End group transformation strategies were studied in the second part of the thesis on linear polymers since characterization of the end groups is more straightforward compared with star polymers. Azide end group modification was achieved while the generation of an amine end group proved to be rather challenging. The introduced azide end group was therefore used to 'click' a Boc protected propargyl amine molecule to the linear polymer via Cu^{I}AAC. The results from the click reaction were positive as well as the removal of the Boc group to yield a primary amine as end group. Nevertheless, several chemical strategies were explored simultaneously to achieve a primary amine as end group directly from bromine. Herein the Gabriel synthesis proved to yield the most successful results. This chemical pathway should be investigated further to minimize the formation of side products. Once optimized these strategies will be translated to star polymers which is expected to be rather straightforward. An azide end group will open doors

towards attachment of several functionalities (e.g. drugs, targeting sequences and imaging probes) while the presence of an amine end group can allow for direct peptide synthesis when the implementation of the thermo-responsive property has been perfected. When both end groups are achieved into one macromolecule, highly versatile star polymers will be realized.

Concerning the applications, preliminary experiments were performed as proof of principle. First the potential on loading of hydrophobic molecules (e.g. hydrophobic dyes or drugs) was examined, showing first promising results on the ability of the star polymer to hold/entrap a hydrophobic dye. This justifies the conduction of future detailed studies on drug entrapment, (controlled) drug release etc. compared with several blind/control tests (using different star polymer compositions). The behavior of the star polymers in complex biological environments on drug release shall be addressed as well. Complex self-assembly behavior of star polymer as well as the critical micelle concentration will also be further investigated. The attachment of MDMO-PPV fluorescent polymers to the star surfaces was also explored in order to extend the use of the system in bio-imaging applications. In this regard purification strategies (recycling GPC) will be employed in the process in order to obtain high purity MDMO-PPV attached star polymers. Hereafter, capacity of the synthesized materials with multifunctional uses (drug carrier, targeted-delivery or bioimaging etc.) will be evaluated in vitro.

Undoubtedly, an important step was made passing and identifying multiple hurdles present in the development of star polymers for biomedical applications. By continuing the development of these polymers the concept will be brought closer towards a theranostic application. Such systems capable of homing onto a specific site or target will definitely improve the outcome of several treatments such as cancer therapies.

References

1. Matyjaszewski, K.; Spanswick, J. *Materials Today* **2005,** *8* (3), 26-33.
2. Braunecker, W. A.; Matyjaszewski, K. *Progress in Polymer Science* **2007,** *32*, 93-146.
3. Nicolas, J.; Guillaneuf, Y.; Lefay, C.; Bertin, D.; Gigmes, D.; Charleux, B. *Progress in Polymer Science* **2013,** (1), 63.
4. Moad, G.; Thang, S. H. *Australian Journal of Chemistry* **2009,** *62* (11), 1379-1381.
5. Matyjaszewski, K.; Tsarevsky, N. V. *Journal of the American Chemical Society* **2014,** *136* (18), 6513-6533.
6. Scholz, C.; Matyjaszewski, K. *Polymer International* **2014,** (5), 801.
7. Matyjaszewski, K.; Patten, T. E.; Xia, J. *Journal of the American Chemical Society* **1997,** *119* (4), 674-680.
8. Gerard, L.; Virgil, P. *Journal of Polymer Science Part A: Polymer Chemistry* **2007,** *45* (20), 4684.
9. Percec, V.; Popov, A. V.; Ramirez-Castillo, E.; Monteiro, M.; Barboiu, B.; Weichold, O.; Asandei, A. D.; Mitchell, C. M. *Journal Of The American Chemical Society* **2002,** *124* (18), 4940-4941.
10. Boyer, C.; Corrigan, N. A.; Jung, K.; Nguyen, D.; Nguyen, T.-K.; Adnan, N. N. M.; Oliver, S.; Shanmugam, S.; Yeow, J. *Chem. Rev.* **2016,** *116* (4), 1803.
11. Frick, E.; Anastasaki, A.; Haddleton, D. M.; Barner-Kowollik, C. *Journal of the American Chemical Society* **2015,** *137* (21), 6889.
12. Anastasaki, A.; Nikolaou, V.; McCaul, N. W.; Simula, A.; Godfrey, J.; Waldron, C.; Wilson, P.; Kempe, K.; Haddleton, D. M. *Macromolecules* **2015,** *48* (5), 1404-1411.
13. Konkolewicz, D.; Schröder, K.; Buback, J.; Bernhard, S.; Matyjaszewski, K. *ACS Macro Letters* **2012,** *1* (10), 1219-1223.
14. Chuang, Y.-M.; Ethirajan, A.; Junkers, T. *ACS Macro Letters* **2014,** *3* (8), 732-737.
15. Mosnáček, J.; Ilčíková, M. *Macromolecules* **2012,** *45* (15), 5859-5865.
16. Wu, W.; Wang, W. G.; Li, J. S. *Progress in Polymer Science* **2015,** *46*, 55-85.
17. Li, Y.; Zhang, B.; Hoskins, J. N.; Grayson, S. M. *Journal of Polymer Science Part A: Polymer Chemistry* **2012,** *50* (6), 1086-1101.
18. Ohno, K.; Wong, B.; Haddleton, D. M. *Journal of Polymer Science Part A: Polymer Chemistry* **2001,** *39* (13), 2206-2214.
19. Waldron, C.; Anastasaki, A.; McHale, R.; Wilson, P.; Li, Z.; Smith, T.; Haddleton, D. M. *Polymer Chemistry* **2014,** *5* (3), 892.
20. Wenn, B.; Martens, A. C.; Chuang, Y. M.; Gruber, J.; Junkers, T. *Polymer Chemistry* **2016,** *7* (15), 2720-2727.
21. Moghimi, S. M.; Hunter, A. C.; Murray, J. C. *FASEB J.* **2005,** *19* (3), 311-30.
22. Wagner, A.; Vorauer-Uhl, K. *Journal of drug delivery* **2011,** *2011*, 591325-9.
23. Johnson, R. P.; Uthaman, S.; John, J. V.; Lee, H. R.; Lee, S. J.; Park, H.; Park, I. K.; Suh, H.; Kim, I. *ACS Appl. Mater. Interfaces* **2015,** *7* (39), 21770-21779.
24. Zhang, W. *Carbohydr. Polym.* **2016,** *139*, 75-81.
25. Hu, Y. F.; Darcos, V.; Monge, S.; Li, S. M. *Int. J. Pharm.* **2015,** *491* (1-2), 152-161.
26. Perez-Herrero, E.; Fernandez-Medarde, A. *European Journal of Pharmaceutics and Biopharmaceutics* **2015,** *93*, 52-79.
27. Gao, H. *Macromol. Rapid Commun.* **2012,** *33* (9), 722.
28. Vancoillie, G.; Frank, D.; Hoogenboom, R. *Progress in Polymer Science* **2014,** *39* (6), 1074-1095.
29. Roy, D.; Brooks, W. L. A.; Sumerlin, B. S. *Chemical Society reviews* **2013,** *42* (17), 7214-7243.
30. Kuckling, D.; Wycisk, A. *Journal of Polymer Science Part A: Polymer Chemistry* **2013,** *51* (14), 2980-2994.
31. Mirshafiee, V.; Mahmoudi, M.; Lou, K.; Cheng, J. *Chem. Commun.* **2013,** *49* (25), 2557-2559.

32. Wu, J.; Zhao, C.; Lin, W. F.; Hu, R. D.; Wang, Q. M.; Chen, H.; Li, L. Y.; Chen, S. F.; Zheng, J. *Journal of Materials Chemistry* **2014,** *2* (20), 2983-2992.
33. Liu, T.; Li, X. J.; Qian, Y. F.; Hu, X. L.; Liu, S. Y. *Biomaterials* **2012,** *33* (8), 2521-2531.
34. Feng, L.; Hu, J.; Liu, Z.; Zhao, F.; Liu, G. *Polymer* **2007,** *48*, 3616-3623.
35. Cheraiet, Z.; Ouarna, S.; Hessainia, S.; Berredjem, M.; Aouf, N.-E. *ISRN organic chemistry* **2012,** *2012*, 404235.
36. Cosemans, I.; Vandenbergh, J.; D'Olieslaeger, L.; Ethirajan, A.; Lutsen, L.; Vanderzande, D.; Junkers, T. *European Polymer Journal* **2014,** *55*, 114-122.
37. Barner-Kowollik, C.; Beuermann, S.; Buback, M.; Castignolles, P.; Charleux, B.; Coote, M. L.; Hutchinson, R. A.; Junkers, T.; Lacík, I.; Russell, G. T.; Stach, M.; van Herk, A. M. *Polymer Chemistry* **2014,** *5* (1), 204.
38. Li, J.; Xiao, H. *Tetrahedron Lett.* **2005,** *46* (13), 2227-2229.
39. Coessens, V.; Nakagawa, Y.; Matyjaszewski, K. *Polym. Bull. (Berlin)* **1998,** *40* (2), 135-142.
40. Vandenbergh, J.; Tura, T.; Baeten, E.; Junkers, T. *Journal of Polymer Science Part A: Polymer Chemistry* **2014,** *52* (9), 1263-1274.
41. Shendage, D. M.; Fröhlich, R.; Haufe, G. *Org. Lett.* **2004,** *6* (21), 3675-3678.
42. Monge, S.; Giani, O.; Ruiz, E.; Cavalier, M.; Robin, J. J. *Macromol. Rapid Commun.* **2007,** *28* (23), 2272-2276.
43. El-Shehawy, A. A.; Sugiyama, K.; Hirao, A. *Reactive and Functional Polymers* **2008,** *68* (12), 1682-1695.
44. Junkers, T.; Wenn, B. *Reaction Chemistry & Engineering* **2016,** *1* (1), 60-64.
45. Kermagoret, A.; Wenn, B.; Debuigne, A.; Jerome, C.; Junkers, T.; Detrembleur, C. *Polym. Chem.* **2015**, 3847-3857.
46. Wenn, B.; Conradi, M.; Carreiras, A. D.; Haddleton, D. M.; Junkers, T. *Polymer Chemistry* **2014,** *5* (8), 3053.
47. Baumann, M.; Baxendale, I. R. *Beilstein J. Org. Chem.* **2015,** *11*, 1194-1219.
48. Radke, W.; Gerber, J.; Wittmann, G. *Polymer* **2003,** *44*, 519-525.
49. Wycisk, A.; Döring, A.; Schneider, M.; Schönhoff, M.; Kuckling, D. *Polymers* **2015,** *7* (5), 921-938.
50. Chmielarz, P.; Park, S.; Sobkowiak, A.; Matyjaszewski, K. *Polymer* **2016,** *88*, 36-42.
51. Zhang, M.; Shen, W.; Xiong, Q.; Wang, H.; Zhou, Z.; Chen, W.; Zhang, Q. *RSC Adv* **2015,** *5* (36), 28133-28140.
52. Anastasaki, A.; Nikolaou, V.; Qiang, Z.; Burns, J.; Samanta, S. R.; Waldron, C.; Haddleton, A. J.; McHale, R.; Fox, D.; Percec, V.; Wilson, P.; Haddleton, D. M. *Journal of the American Chemical Society* **2014,** *136* (3), 1141-1149.
53. Mauricio, M. R.; Otsuka, I.; Borsali, R.; Petzhold, C. L.; Cellet, T. S. P.; Carvalho, G. M. d.; Rubira, A. F. *Reactive and Functional Polymers* **2011,** *71* (12), 1160-1165.
54. Chang, C.-W.; Bays, E.; Tao, L.; Alconcel, S. N. S.; Maynard, H. D. *Chem. Commun.* **2009,** (24), 3580-3582.
55. Li, B.; Bemish, R.; Buzon, R. A.; Chiu, C. K. F.; Colgan, S. T.; Kissel, W.; Le, T.; Leeman, K. R.; Newell, L.; Roth, J. *Tetrahedron Lett.* **2003,** *44* (44), 8113-8115.
56. Corey, E.; Link, J. O. *Journal of the American Chemical Society* **1992,** *114* (5), 1906-1908.
57. Coessens, V.; Pintauer, T.; Matyjaszewski, K. *Progress in Polymer Science* **2001,** *26* (3), 337-377.
58. Li, X.; Qian, Y.; Liu, T.; Liu, S.; Hu, X.; Zhang, G.; You, Y. *Biomaterials* **2011,** *32* (27), 6595-6605.
59. Abulateefeh, S. R.; Spain, S. G.; Aylott, J. W.; Chan, W. C.; Garnett, M. C.; Alexander, C. *Macromol. Biosci.* **2011,** *11* (12), 1722-1734.
60. Gidwani, B.; Vyas, A. *BioMed Research International* **2015,** *2015*, 198268.
61. Karukstis, K. K.; Thompson, E. H. Z.; Whiles, J. A.; Rosenfeld, R. J. *Biophys. Chem.* **1998,** *73* (3), 249-263.
62. Zaquen, N.; Lu, H.; Chang, T.; Mamdooh, R.; Lutsen, L.; vanderzande, D.; Stenzel, M.; Junkers, T. *Chem. Sci.* **Submitted**.

63. Peters, M.; Zaquen, N.; D'Olieslaeger, L.; Bové, H.; vanderzande, D.; Hellings, N.; Junkers, T.; Ethirajan, A. *Biomacromolecules* **in press**.

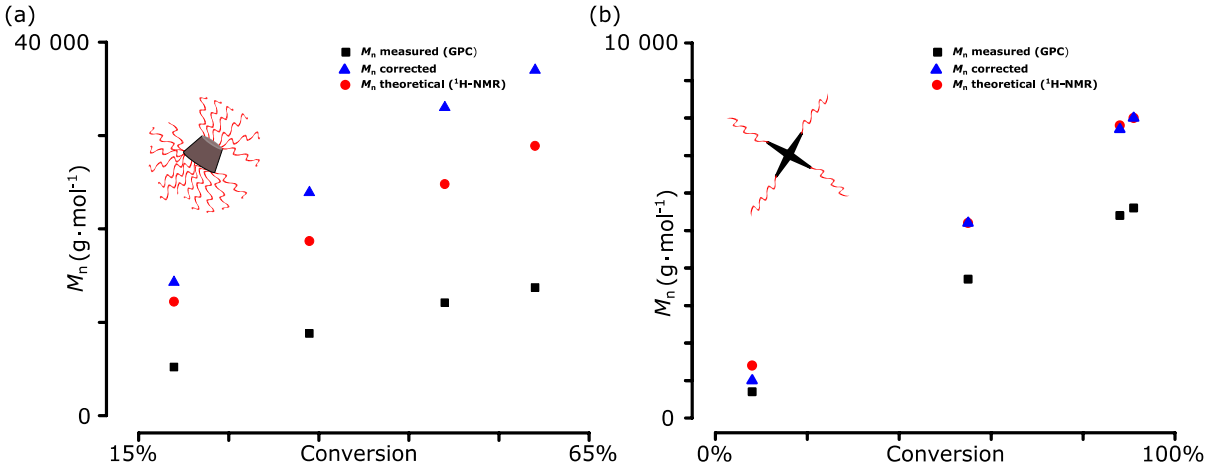

SI 1: Demonstration of effect of the correction factor on 21- (a) and 4-arm star polymers (b). The M_n was measured by GPC (■), the value was corrected with a literature known value (2.73 and 1.42 for 21-and 4-arm star polymers respectively, ▲)[48]. The theoretical value was calculated via conversion by ^{1}H-NMR (●). 4-arm star polymers were synthesized following a literature procedure.[20]

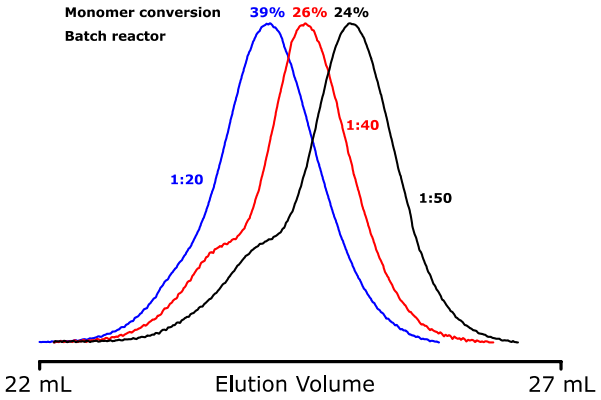

SI 2: The effect of dilution on star polymers synthesized in the batch reactor. Reactions were performed for 45 minutes and arm lengths were targeted for 15 000 g·mol^{-1}. The [CH-Br]:[Cu^{II}Br$_2$]:[Me$_6$TREN]:[MA]/[DEGA] equivalents used were 1:0.01:0.075:174. The used monomer to solvent (DMSO) dilutions were 1:20, 1:40 and 1:50.

(a)

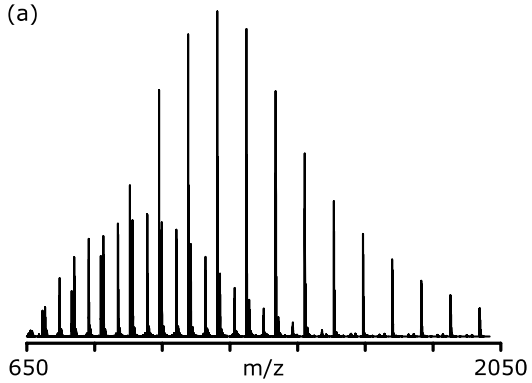

(b)

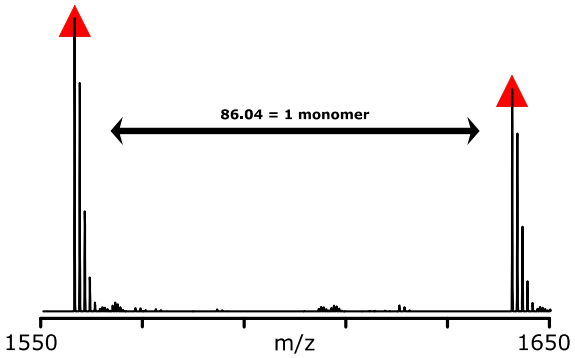

(c)

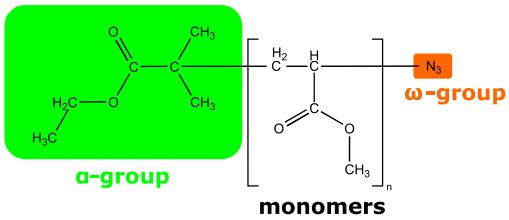

(d)

α-group	ω-group	Number of monomers	Ion	$m/z_{, th}$	$m/z_{, exp}$
▲ EBiB	N_3	15	**Na^+**	1556.66	1556.66
▲ EBiB	N_3	16	**Na^+**	1642.70	1642.70

SI 3: Full ESI-MS spectrum (a) and spectrum of single monomer repeating units (b) of azide end group modified linear polymer (c). Triangles represent single charged species. The different theoretical and experimental m/z values are given in (d). The azide end group was introduced in the linear polymer using [CH-Br]:[NaN_3] equivalents of 1:2 by stirring for 5 hours at room temperature.

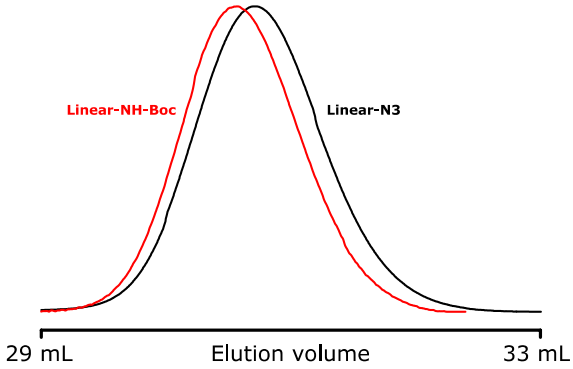

SI 4: GPC traces of the linear polymer after Cu^IAAC with *N*-Boc-propargylamine. The starting polymer is represented by a black curve while a red one represents *N*-Boc-propargylamine functionalized polymer. Cu^IAAC was performed using [CH-N_3]:[Cu^IBr]:[PMDETA]:[*N*-Boc propargylamine] equivalents of 1:2:4:2 by stirring overnight at room temperature under nitrogen atmosphere.

(a)

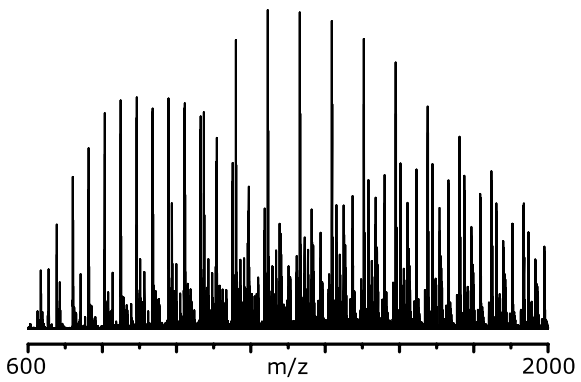

(b)

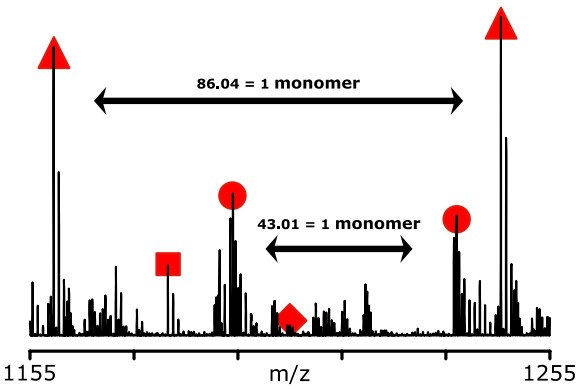

(c)

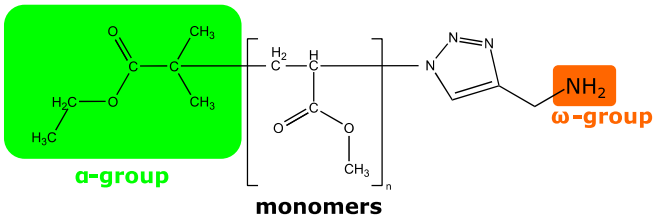

(d)

α-group	ω-group	Number of monomers	Ion	$m/z_{, th}$	$m/z_{, exp}$
▲ EBiB	NH_2	10	H^+	1159.54	1159.54
▲ EBiB	NH_2	11	H^+	1245.58	1245.58
● EBiB	NH_2	24	$Na^+ + H^+$	1193.52	1194.03
● EBiB	NH_2	25	$Na^+ + H^+$	1236.54	1237.04
■ EBiB	NH_2	10	Na^+	1181.52	1181.53
◆ EBiB	NH_2	24	$2Na^+$	1204.52	1204.52

SI 5: Full ESI-MS spectrum (a) and spectrum of single monomer repeating units (b) of propargylamine modified linear polymers after TFA treatment (c). The different theoretical and experimental m/z values are given in (d). The protecting Boc group was removed by stirring with an excess of trifluoroacetic acid at room temperature overnight.

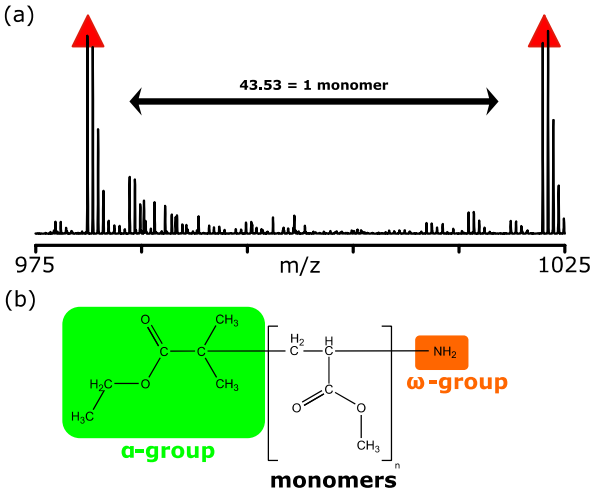

(c)

α-group	ω-group	Number of monomers	Ion	$m/z_{, th}$	$m/z_{, exp}$
▲ EBiB	NH_2	20	$Na^+ + H^+$	980.93	979.89
▲ EBiB	NH_2	21	$Na^+ + H^+$	1023.95	1023.42

SI 6: Full ESI-MS spectrum of amine end group modified linear polymers after hydrazinolysis. The major distribution belongs to double charged amine end group modified linear polymers. Hydrazinolysis was performed using [CH-phtalamide]:[hydrazine monohydrate] equivalents of 1:5 by refluxing for 24 hours at 55 °C.

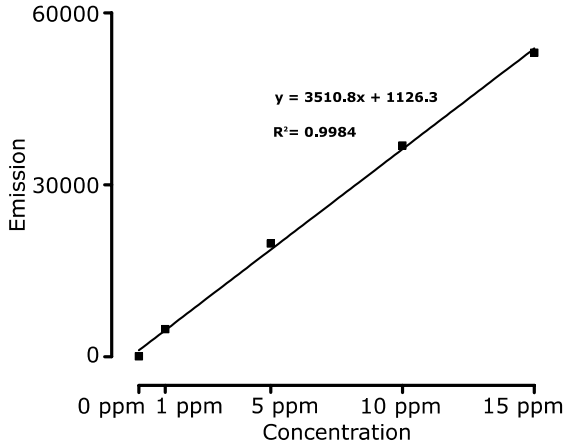

SI 7: Rhodamine B dodecyl ester standard calibration curve. The standard solutions containing different concentrations, ranging from 0 ppm to 15 ppm of fluorescent dye were prepared in ethanol.

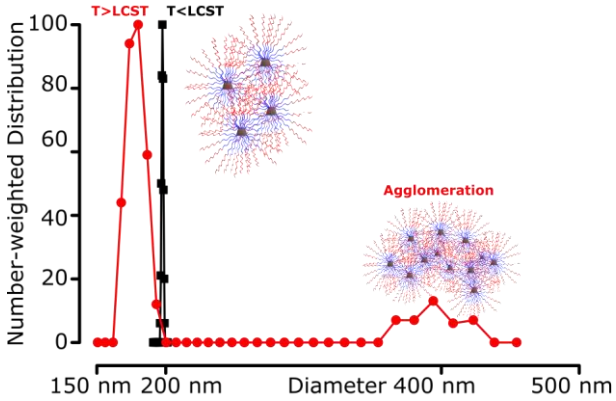

SI 8: Observation of agglomeration behavior of star polymer P3 (M_n = 590 600 g·mol^{-1}, Đ = 1.15) by DLS with a concentration of 0.1 wt% in H_2O. Black line represents the number weighted distributions of star polymer with a temperature below LCST, where the red-line represents the particle distribution above the LCST.

SI 9: Emission values after excitation of azide and MDMO-PPV end group modified star polymers. The samples were excited at 485 nm with a gain of 750. Emission values were recorded at 590 nm.

End group	**Emission**, λ = 590 nm
Azide	58
MDMO-PPV	1333

Auteursrechtelijke overeenkomst

Ik/wij verlenen het wereldwijde auteursrecht voor de ingediende eindverhandeling:
Star polymers for biomedical application

Richting: **master in de biomedische wetenschappen-bio-elektronica en nanotechnologie**
Jaar: **2016**

in alle mogelijke mediaformaten, - bestaande en in de toekomst te ontwikkelen - , aan de Universiteit Hasselt.

Niet tegenstaand deze toekenning van het auteursrecht aan de Universiteit Hasselt behoud ik als auteur het recht om de eindverhandeling, - in zijn geheel of gedeeltelijk -, vrij te reproduceren, (her)publiceren of distribueren zonder de toelating te moeten verkrijgen van de Universiteit Hasselt.

Ik bevestig dat de eindverhandeling mijn origineel werk is, en dat ik het recht heb om de rechten te verlenen die in deze overeenkomst worden beschreven. Ik verklaar tevens dat de eindverhandeling, naar mijn weten, het auteursrecht van anderen niet overtreedt.

Ik verklaar tevens dat ik voor het materiaal in de eindverhandeling dat beschermd wordt door het auteursrecht, de nodige toelatingen heb verkregen zodat ik deze ook aan de Universiteit Hasselt kan overdragen en dat dit duidelijk in de tekst en inhoud van de eindverhandeling werd genotificeerd.

Universiteit Hasselt zal mij als auteur(s) van de eindverhandeling identificeren en zal geen wijzigingen aanbrengen aan de eindverhandeling, uitgezonderd deze toegelaten door deze overeenkomst.

Voor akkoord,

Vrijsen, Jeroen

Datum: **8/06/2016**